Probability distributions of wind speed in the UAE

T.B.M.J. Ouarda[1, 2*], C. Charron[1], J.-Y. Shin[1], P.R. Marpu[1], A.H. Al-Mandoos[3], M.H. Al-Tamimi[3], H. Ghedira[1] and T.N. Al Hosary[3]

[1]Institute Center for Water and Environment (iWATER), Masdar Institute of Science and Technology, P.O. Box 54224, Abu Dhabi, UAE

[2]INRS-ETE, National Institute of Scientific Research, 490 de la Couronne, Quebec City (QC), Canada, G1K9A9

[3]National Centre of Meteorology and Seismology, P.O. Box 4815, Abu Dhabi, UAE

*Corresponding author:

Email: touarda@masdar.ac.ae

Tel: +971 2 810 9107

Submitted to Energy Conversion and Management

December 2014

Abstract

For the evaluation of wind energy potential, probability density functions (pdfs) are usually used to describe wind speed distributions. The selection of the appropriate pdf reduces the wind power estimation error. The most widely used pdf for wind energy applications is the 2-parameter Weibull probability density function. In this study, a selection of pdfs are used to model hourly wind speed data recorded at 9 stations in the United Arab Emirates (UAE). Models used include parametric models, mixture models and one non-parametric model using the kernel density concept. A detailed comparison between these three approaches is carried out in the present work. The suitability of a distribution to fit the wind speed data is evaluated based on the log-likelihood, the coefficient of determination R^2, the Chi-square statistic and the Kolmogorov-Smirnov statistic. Results indicate that, among the one-component parametric distributions, the Kappa and Generalized Gamma distributions provide generally the best fit to the wind speed data at all heights and for all stations. The Weibull was identified as the best 2-parameter distribution and performs better than some 3-parameter distributions such as the Generalized Extreme Value and 3-parameter Lognormal. For stations presenting a bimodal wind speed regime, mixture models or non-parametric models were found to be necessary to model adequately wind speeds. The two-component mixture distributions give a very good fit and are generally superior to non-parametric distributions.

Keywords

probability density function; model selection criteria; wind speed distribution; Kappa distribution; coefficient of determination; mixture distribution; non-parametric model.

1 Introduction

The characterization of short term wind speeds is essential for the evaluation of wind energy potential. Probability density functions (pdfs) are generally used to characterize wind speed observations. The suitability of several pdfs has been investigated for a number of regions in the world. The choice of the pdf is crucial in wind energy analysis because wind power is formulated as an explicit function of wind speed distribution parameters. A pdf that fits more accurately the wind speed data will reduce the uncertainties in wind power output estimates.

The 2-parameter Weibull distribution (W2) and the Rayleigh distribution (RAY) are the pdfs that are the most commonly used in wind speed data analysis especially for studies related to wind energy estimation (Justus et al., 1976; Hennessey, 1977; Nfaoui et al., 1998; Sahin and Aksakal, 1998; Persaud et al. 1999; Archer and Jacobson, 2003; Celik, 2003; Fichaux and Ranchin, 2003; Kose et al., 2004; Akpinar and Akpinar, 2005; Ahmed Shata and Hanitsch, 2006; Acker et al., 2007; Gökçek et al., 2007; Mirhosseini et al., 2011; Ayodele et al., 2012; Irwanto et al., 2014; Ordonez et al., 2014; Petković et al., 2014). The W2 is by far the most widely used distribution to characterize wind speed. The W2 was reported to possess a number of advantages (Tuller and Brett, 1985, for instance): it is a flexible distribution; it gives generally a good fit to the observed wind speeds; the pdf and the cumulative distribution function (cdf) can be described in closed form; it only requires the estimation of 2 parameters; and the estimation of the parameters is simple. The RAY, a one parameter distribution, is a special case of the W2 when the shape parameter of this latter is set to 2. It is most often used alongside the W2 in studies related to wind speed analysis (Hennessey, 1977; Celik, 2003; Akpinar and Akpinar, 2005).

Despite the fact that the W2 is well accepted and provides a number of advantages, it cannot represent all wind regimes encountered in nature, such as those with high percentages of null wind speeds, bimodal distributions, etc. (Carta et al., 2009). Consequently, a number of other models have been proposed in the literature including standard distributions, non-parametric models, mixtures of distributions and hybrid distributions. A 3-parameter Weibull (W3) model with an additional location parameter has been used by Stewart and Essenwanger (1978) and Tuller and Brett (1985). They concluded to a general better fit with the W3 instead of the ordinary W2. Auwera et al. (1980) proposed the use of the Generalized Gamma distribution (GG), a generalization of the W2 with an additional shape parameter, for the estimation of mean wind power densities. They found that it gives a better fit to wind speed data than several other distributions. Recently, a variety of other standard pdfs have been used to characterize wind speed distributions (Carta et al., 2009; Zhou et al., 2010; Lo Brano et al., 2011; Morgan et al., 2011; Masseran et al., 2012; Soukissian, 2013). These include the Gamma (G), Inverse Gamma (IG), Inverse Gaussian (IGA), 2 and 3-parameter Lognormal (LN2, LN3), Gumbel (EV1), 3-parameter Beta (B), Pearson type III (P3), Log-Pearson type III (LP3), Burr (BR), Erlang (ER), Kappa (KAP) and Wakeby (WA) distributions. Some studies considered non-stationary distributions in which the parameters evolve as a function of a number of covariates such as time or climate oscillation indices (Hundecha et al., 2008). This approach allows integrating in the distributional modeling of wind speed information concerning climate variability and change.

To account for bimodal wind speed distributions, mixture distributions have been proposed by a number of authors (Carta and Ramirez, 2007; Akpinar and Akpinar, 2009; Carta et al., 2009; Chang, 2011; Qin et al., 2012). The common models used are a mixture of two W2 and a mixture of a normal distribution singly truncated from below with a W2 distribution. In Carta et al.

(2009), the mixture models were found to provide a good fit for bimodal wind regimes. They were also reported to provide the best fits for unimodal wind regimes compared to standard distributions.

Non-parametric models were also proposed by a number of authors. The most popular are distributions generated by the maximum entropy principle (Li and Li, 2005; Ramirez and Carta, 2006; Akpinar and Akpinar, 2007; Chang, 2011; Zhang et al., 2014). These distributions are very flexible and have the advantage of taking into account null wind speeds. Another non-parametric model using the kernel density concept was proposed by Qin et al. (2011). This approach was applied by Zhang et al. (2013) in a multivariate framework.

Because a minimal threshold wind speed is required to be recorded by an anemometer, null wind speeds are often present. However, for many distributions, including the W2, null wind speeds or calm spells are not properly accounted for because the cdf of these distributions gives a null probability of observing null wind speeds (i.e. $F_X(0)=0$, where $F_X(x)$ is the cdf of a given variable *X*). Takle and Brown (1978) introduced what they called the "hybrid density probability" to consider null wind speeds. The zero values are first removed from the time series and a distribution is fitted to the non-zero series. The zeros are then reintroduced to give the proper mean and variance and renormalize the distribution. Carta et al. (2009) applied hybrid functions with several distributions and concluded that there is no indication that hybrid distributions offer advantages over the standard ones.

In order to compare the goodness-of-fit of various pdfs to sample wind speed data, several statistics have been used in studies related to wind speed analysis. The most frequently used ones are the coefficient of determination (R^2) (Garcia et al., 1998; Celik, 2004; Akpinar and Akpinar, 2005; Li and Li, 2005; Ramirez and Carta, 2006; Carta et al., 2009; Morgan et al., 2011; Soukissian, 2013; Zhang et al., 2013), the Chi-square test results (χ^2) (Auwera et al., 1980; Conradsen et al., 1984; Dorvlo, 2002; Akpinar and Akpinar, 2005; Chang, 2011), the Kolmogorov-Smirnov test results (KS) (Justus et al., 1976, 1978; Tuller and Brett, 1985; Poje and Cividini, 1988; Dorvlo, 2002; Chang, 2011; Qin et al., 2011; Usta and Kantar, 2012) and the root mean square error (rmse) (Justus et al., 1976, 1978; Auwera et al., 1980; Seguro and Lambert, 2000; Akpinar and Akpinar, 2005; Chang, 2011). In most studies, a visual assessment of fitted pdfs superimposed on the histograms of wind speed data is also performed (Nfaoui et al., 1998; Algifri, 1998; Ulgen and Hepbasli, 2002; Archer and Jacobson, 2003; Kose et al. 2004; Jaramillo et al., 2004; Chang, 2011; Qin et al., 2011; Chellali et al., 2012). R^2 and rmse are either applied on theoretical cumulative probabilities against empirical cumulative probabilities (P-P plot) (Ramirez and Carta, 2006; Carta et al., 2009; Morgan et al., 2011; Soukissian, 2013) or on theoretical wind speed quantiles against observed wind speed quantiles (Q-Q plot) (Garcia et al., 1998; Celik, 2004; Akpinar and Akpinar, 2005; Li and Li, 2005; Zhang et al., 2013). These statistics are also sometimes computed with wind speed data in the form of frequency histograms (Carta et al., 2008, 2009; Zhou et al., 2010; Qin et al., 2011; Usta and Kantar, 2012).

In addition to the analysis performed on wind speed distributions, some authors have also evaluated the suitability of pdfs to fit the power distributions obtained by sample wind speeds or to predict the energy output (Auwera et al.,1980; Seguro and Lambert, 2000; Celik, 2004; Li and Li, 2005; Gökçek et al., 2007; Zhou et al., 2010; Chang, 2011; Morgan et al., 2011; Chellali et al., 2012). In this case, pdfs are first fitted to the wind speed data. Then, theoretical power density distributions are derived from the pdfs fitted to wind speed. Finally, measures of goodness-of-fit are computed using the theoretical wind power density distributions and the estimated power distribution from sample wind speeds. Alternatively, analyses are also performed on the cube of wind speed which is proportional to the wind power (Hennessey et al., 1977; Carta et al., 2009).

A relatively limited number of studies have been conducted on the assessment of pdfs to model wind speed distributions in the Arabian Peninsula or neighboring regions: Algifri (1998) in Yemen, Mirhosseini (2011) in Iran, Sulaiman et al. (2002) in Oman, and Şahin and Aksakal (1998) in Saudi Arabia. In all these studies, only the W2 or the RAY has been used.

The aim of the present study is to evaluate the suitability of a large number of pdfs, commonly used to model hydro-climatic variables, to characterize short term wind speeds recorded at meteorological stations located in the United Arab Emirates (UAE). A comparison among one-component parametric models, mixture models and a non-parametric model is carried out. The one-component parametric distributions selected are the EV1, W2, W3, LN2, LN3, G, GG, Generalized Extreme Value (GEV), P3, LP3 and KAP. The mixture models considered in this work are the two-component mixture Weibull distribution (MWW) and the two-component mixture Gamma distribution (MGG). For the non-parametric approach, a distribution using the kernel density concept is considered. The evaluation of the goodness-of-fit of the pdfs to the data is carried out through the use of the log-likelihood (ln L), R^2, χ^2 and KS. The present paper is organized as follows: Section 2 presents the wind speed data used. Section 3 illustrates the methodology. The study results are presented in Section 4 and the conclusions are presented in Section 5.

2 Wind speed data

The UAE is located in the south-eastern part of the Arabian Peninsula. It is bordered by the Arabian Sea and Oman in the east, Saudi Arabia in the south and west and the Gulf in the north. The climate of the UAE is arid with hot summers. The coastal area has a hot and humid summer with temperatures and relative humidity reaching 46 °C and 100% respectively. The interior desert region has very hot summers with temperatures rising to about 50 °C and cool winters during which the temperatures can fall to around 4 °C (Ouarda et al., 2014).Wind speeds in the UAE are generally below 10 m/s for most of the year. Strong winds with mean speeds exceeding 10 m/s over land areas occur in association with a weather system, such as an active surface trough or squall line. Occasional strong winds also occur locally during the passage of a gust front associated with a thunderstorm. Strong north-westerly winds often occur ahead of a surface trough and can reach speeds of 10-13 m/s, but usually do not last more than 6-12 hours. On the passage of the trough, the winds veer south-westerly with speeds of up to 20 m/s over the sea, but rarely exceed 13 m/s over land.

Wind speed data comes from 9 meteorological stations located in the UAE. Table 1 gives a description of the stations including geographical coordinates, altitude, measuring height and period of record. For 7 of the 9 stations, only one anemometer is available and it is located at a height of 10 m. For the 2 others, there are anemometers at different heights. Periods of record range from 11 months to 39 months. The geographical location of the stations is illustrated in Figure 1. It shows that the whole country is geographically well represented. 4 stations (Sir Bani Yas Island, Al Mirfa, Masdar city and Masdar Wind Station) are located near the coastline. The stations of East of Jebel Haffet and Al Hala are located in the mountainous north-eastern region. The station of Al Aradh is location in the foothills and the stations of Al Wagan and Madinat

Zayed are located inland. Masdar Wind Station is located approximately at the same position than the station of Masdar City.

Wind speed data were collected initially by anemometers at 10-min intervals. Average hourly wind speed series, which is the most common time step used for characterizing short term wind speeds, are computed from the 10-min wind speed series. Missing values, represented by extended periods of null hourly wind speed values, were removed from the hourly series. Percentages of calms for the hourly time series of this study are extremely low.

3 Methodology

3.1 One-component parametric probability distributions

A selection of 11 distributions was fitted to the wind speed series of this study. Table 2 presents the pdfs of all distributions with their domain and number of parameters. For each pdf, one or more methods were used to estimate the parameters. Methods used for each pdf are listed in Table 2. For most distributions, the maximum likelihood method (ML) and the method of moments (MM) were used. For KAP, the method of L-moments (LM) was applied instead of MM. Singh et al. (2003) showed that a better fit is obtained when the parameters of KAP are estimated with LM instead of MM. The LM method is described in Hosking and Wallis (1997) and the algorithm used is presented in Hosking (1996). For the LP3, the Generalized Method of Moments (GMM) (see Bobée, 1975, and Ashkar and Ouarda, 1996) as well as two of its variants, the method of the Water Resources Council (WRC) from the Water Resources Council (1967) and the Sundry Averages Method (SAM) from Bobée and Ashkar (1988) were used. Results obtained in this study reveal that GMM gave a significantly superior fit than the other methods and consequently only the results obtained with this method are presented here.

3.2 Mixture probability distributions

To model wind regimes presenting bimodality, it is common to use models with a linear combination of distributions. Suppose that V_i (i = 1, 2, …, d) are independently distributed with d distributions $f(v;\theta_i)$ where θ_i are the parameters of the i^{th} distribution. The mixture density function of V distributed as V_i with mixing parameters ω_i is said to be a d component mixture distribution where $\sum_{i=1}^{d}\omega_i = 1$. The mixture density function of V is given by:

$$f(v;\omega,\theta) = \sum_{i=1}^{d}\omega_i f_i(v;\theta_i)\,. \tag{1}$$

In the case of a two-component mixture distribution, the mixture density function is then:

$$f(v;\omega,\theta_1,\theta_2) = \omega f(v;\theta_1) + (1-\omega) f(v;\theta_2)\,. \tag{2}$$

Mixture of two 2-parameter Weibull pdfs (MWW) and two Gamma pdfs (MGG) are used in this study. The probability density functions of these two mixture models are presented in Table 2. The least-square method (LS) is used to fit the parameters of both mixture models. This method is largely employed with mixture distributions applied to wind speeds (Carta and Ramirez, 2007; Akpinar and Akpinar, 2009). The least-square function is optimized with a genetic algorithm. Advantages of the genetic algorithm are that it is more likely to reach the global optimum and it does not require defining initial values for the parameters, which is difficult in the case of mixture distributions.

3.3 Non-parametric kernel density

For a data sample, $x_1,\ldots,x_n$, the kernel density estimator is defined by:

$$\hat{f}(x;h) = \frac{1}{nh}\sum_{i=1}^{n} K\left(\frac{x - x_i}{h}\right) \quad (3)$$

where K is the kernel function and h is the bandwidth parameter. The kernel function selected for this study is the Gaussian function given by:

$$K\left(\frac{x - x_i}{h}\right) = \left(\frac{1}{\sqrt{2\pi}}\right)\exp\left(-\frac{(x - x_i)^2}{2h^2}\right). \quad (4)$$

The choice of the bandwidth parameter is a crucial factor as it controls the smoothness of the density function. The mean integrated squared error (MISE) is commonly used to measure the performance of $\hat{f}$:

$$\mathrm{MISE}(h) = E\int\left(\hat{f}(x,h) - f(x)\right)^2 dx\ . \quad (5)$$

MISE is approximated by the asymptotic mean integrated squared error (AMISE; Jones et al., 1996):

$$AMISE\,(\mathrm{h}) = n^{-1}h^{-1}R(K) + h^4 R(f'')\left(\int x^2 K / 2\right) \quad (6)$$

where $R(\varphi) = \int \varphi^2(x)dx$ and $\int x^2 K = \int x^2 K(x)dx$. The optimal bandwidth parameter that optimizes Eq. (6) is:

$$h_{AMISE} = \left[\frac{R(K)}{nR(f'')(\int x^2 K)^2}\right]. \quad (7)$$

In this study, Eq. (7) is solved with the R package kedd (Guidoum, 2014).

3.4 Assessment of goodness-of-fit

To evaluate the goodness-of-fit of the pdfs to the wind speed data, the ln L, two variants of the R^2, the χ^2 and the KS were used. A number of approaches to compute the R^2 statistic are found in the literature and are considered in this study. Thus, two variants of R^2 are computed: R^2_{PP} which uses the P-P probability plot approach and R^2_{QQ} which uses the Q-Q probability plot approach. These indices are described in more detail in the following subsections.

3.4.1 log-likelihood (ln *L*)

ln L measures the goodness-of-fit of a model to a data sample. For a given pdf $f_{\hat{\theta}}(x)$ with distribution parameter estimates $\hat{\theta}$, it is defined by:

$$\ln L = \ln\left(\prod_{i=1}^{n} f_{\hat{\theta}}(v_i)\right) \tag{8}$$

where v_i is the i^{th} observed wind speed and n is the number of observations in the data set. A higher value of this criterion indicates a better fit of the model to the data. It should be noted that ln L cannot always be calculated for the LP3 and KAP distributions. The reason is that it occasionally happens that at least one wind speed observation is outside the domain defined by the distribution for the parameters estimated by the given estimation method. Then, at least one probability density of zero is obtained which makes the calculation of the log-likelihood impossible.

3.4.2 R^2_{PP}

R_{PP}^2 is the coefficient of determination associated with the P-P probability plot which plots the theoretical cdf versus the empirical cumulative probabilities. R_{PP}^2 quantifies the linear relation between predicted and observed probabilities. It is computed as follows:

$$R_{PP}^2 = 1 - \frac{\sum_{i=1}^{n}(F_i - \hat{F}_i)^2}{\sum_{i=1}^{n}(F_i - \bar{F})^2} \tag{9}$$

where $\hat{F}_i$ is the predicted cumulative probability of the i^{th} observation obtained with the theoretical cdf, F_i is the empirical probability of the i^{th} observation and $\bar{F} = \frac{1}{n}\sum_{i=1}^{n} F_i$. The empirical probabilities are obtained with the Cunnane (1978) formula:

$$F_i = \frac{i - 0.4}{n + 0.2} \tag{10}$$

where $i = 1,...,n$ is the rank for ascending ordered observations. An example of a P-P plot is presented in Figure 2a for KAP/LM at the station of East of Jebel Haffet.

3.4.3 R_{QQ}^2

R_{QQ}^2 is the coefficient of determination associated with the Q-Q probability plot defined by the predicted wind speed quantiles obtained with the inverse function of the theoretical cdf versus the observed wind speed data. Plotting positions for estimated quantiles are given by the empirical probabilities F_i defined previously. R_{QQ}^2 quantifies the linear relation between predicted and observed wind speeds and is computed as follows:

$$R_{QQ}^2 = 1 - \frac{\sum_{i=1}^{n}(v_i - \hat{v}_i)^2}{\sum_{i=1}^{n}(v_i - \bar{v})^2} \tag{11}$$

where $\hat{v}_i = F^{-1}(F_i)$ is the i^{th} predicted wind speed quantile for the theoretical cdf $F(x)$, v_i is the i^{th} observed wind speed and $\bar{v} = \frac{1}{n}\sum_{i=1}^{n} v_i$. An example of a Q-Q plot is presented in Figure 2b for KAP/LM at the station of East of Jebel Haffet.

3.4.4 Chi-square test (χ^2)

The Chi-square goodness-of-fit test judges the adequacy of a given theoretical distribution to a data sample. The sample is arranged in a frequency histogram having N bins. The Chi-square test statistic is given by:

$$\chi^2 = \sum_{i=1}^{N} \frac{(O_i - E_i)^2}{E_i} \tag{12}$$

where O_i is the observed frequency in the i^{th} class interval and E_i is the expected frequency in the i^{th} class interval. E_i is given by $F(v_i) - F(v_{i-1})$ where v_{i-1} and v_i are the lower and upper limits of the i^{th} class interval. The size of class intervals chosen in this study is 1 m/s. A minimum expected frequency of 5 is required for each bin. When an expected frequency of a class interval is too small, it is combined with the adjacent class interval. This is a usual procedure as a class interval with an expected frequency that is too small will have too much weight.

3.4.5 Kolmogorov-Smirnov (KS)

The KS test computes the largest difference between the cumulative distribution function of the model and the empirical distribution function. The KS test statistic is given by:

$$D = \max_{1 \le i \le n} \left| F_i - \hat{F}_i \right| \quad (13)$$

where $\hat{F}_i$ is the predicted cumulative probability of the i^{th} observation obtained with the theoretical cdf and F_i is the empirical probability of the i^{th} observation obtained with Eq. (10).

4 Results

Each selected pdf was fitted to the wind speed series with the different methods and the statistics of goodness-of-fit were afterwards calculated. The results are presented here separately for stations with an anemometer at the 10 m height and for stations with anemometers at other heights.

4.1 Description of wind speed data

Table 3 presents the descriptive statistics of each station including maximum, mean, median, standard deviation, coefficient of variation, coefficient of skewness and coefficient of kurtosis. For stations at 10 m, mean wind speeds vary from 2.47 m/s to 4.28 m/s. The coefficients of variation are moderately low, ranging from 0.46 to 0.7. All coefficients of skewness are positive, indicating that all distributions are right skewed. The coefficients of kurtosis are moderately high, ranging from 2.9 to 4.47.

Figures 3 and 4 present respectively the spatial distribution of the median wind speed and the altitude of the stations at 10 m. The circle sizes in Figures 3 and 4 are respectively proportional to the median wind speeds and the altitudes of stations. Generally, coastal sites (Sir Bani Yas Island, Al Mirfa and Masdar City) and sites near the mountainous region (East of Jebel Haffet) are subject to higher mean wind speeds than inland sites. Two of the coastal sites of this study have high wind speeds. However, Masdar City is characterized by lower wind speeds.

Altitude is an important factor to explain wind speeds. For this study, the largest median wind speed occurs at East of Jebel Haffet, which is also the station that is located at the highest altitude (341 m) among the 10 m height stations. However, Al Aradh, also located at a relatively high altitude (178 m), has the lowest median wind speed. This shows that a diversity of other factors affect wind speeds and a simple relation between mean values and geophysical characteristics is difficult to establish. It is necessary to study in detail the effects of other factors such as large-scale and small-scale features, terrain characteristics, presence of obstacles, surface roughness, presence of ridges and ridge concavity in the dominant windward direction, and channeling effect.

4.2 Stations at 10 m height

Table 4 presents the goodness-of-fit statistics for each distribution associated with a method (D/M) for the stations at 10 m height. Since R_{PP}^2, R_{QQ}^2, χ^2 and KS allow comparing different samples together, the statistics obtained are presented with box plots in Figure 5. LN2 leading to poor fits has been discarded from these box plots. Table 5 lists the 6 best D/Ms based on all goodness-of-fit statistics. The best one-component parametric pdfs are denoted with superscript letter a and the best two-component mixture parametric pdfs are denoted with superscript letter b in Table 5. The performances of one-component parametric models are first analyzed here and the comparison with mixture models and the non-parametric model is carried out afterwards.

The box plots of statistics in Figure 5 are used to analyze the performances of one-component parametric pdfs. Based on R_{PP}^2, KAP/LM leads to the best fits followed closely by GG/MM.

Based on R^2_{QQ}, GG/MM is the best D/M followed closely by KAP/LM. Based on χ^2, GG/MM leads to the best fit followed closely by W3/ML. Finally, based on KS, KAP/LM is the best D/M followed by GG/MM. With all statistics considered in this study, the W2 is the best 2-parameter distribution and leads to better performances than the 3-parameter distributions GEV and LN3. Box plots reveal also that D/Ms using MM are somewhat preferred over those that use ML.

Ranks of one-component parametric models in Table 5 are analyzed here. Based on ln *L*, KAP/ML and GG/ML are the best D/Ms for 3 stations. Even if GG is often one of the best ranked pdf, it is not even included among the best pdfs for the stations of Al Mirfa, East of Jebel Haffet and Madinat Zayed. On the other hand, the KAP is included within the best D/Ms for all 7 stations. It is important also to notice that D/Ms using ML, a method that maximizes the log-likelihood function, are preferred by ln *L* over D/Ms using other methods. For R^2_{PP}, the KAP/LM is the best D/M for 5 stations. GG, being the second best pdf, is not even among the best 6 D/Ms for most stations. Based on the R^2_{QQ} statistic, GG/MM is the best D/M for 4 stations and is ranked the overall third best for two other stations. However, GG is not listed among the best D/Ms for the station of East-of-Jebel Haffet, while KAP/LM is within the best D/Ms for all stations. Based on χ^2, GG/MM is the best D/M for 4 stations in Table 5. However, GG is not within the best 6 D/Ms for East of Jebel Haffet. Based on KS, KAP/LM is the best D/M for 5 stations and is among the 6 best D/Ms for every station. GG, the second best pdf, is not within the best 6 D/Ms for East of Jebel Haffet, Madinat Zayed and Sir Bani Yas Island.

Globally, the best performances for one-component parametric models are obtained with the KAP and GG. For R^2_{PP} and KS, KAP is clearly the preferred distribution. For ln *L*, R^2_{QQ} and χ^2, either KAP or GG can be considered as the preferred distribution. However, the GG distribution is less flexible. Indeed, GG is often not selected among the 6 best D/Ms.

Mixture distributions MWW/LS and MGG/LS are among the distributions giving the best fits with respect to box plots of statistics. For instance, MWW/LS is the best overall model according to R_{PP}^2 and KS. MWW/LS performs very well for most stations with respect to χ^2. However, the box plot for MWW/LS reveals the presence of an outlier (Madinat Zayed) for this statistic. MWW/LS gives generally better fits than MGG/LS according to every statistic.

Results in Table 5 show that, according to ln L, MWW/LS is not within the best 6 D/Ms for 3 stations. MWW/LS is ranked first for 5 stations based on R_{PP}^2. Based on R_{QQ}^2, MWW/LS is the best D/M for 3 stations but is not ranked within the best 6 D/Ms for 3 other stations. Based on χ^2, MWW/LS is the best parametric model for 4 stations. Based on KS, it is ranked first for 4 stations and is ranked second otherwise.

According to ln L, R_{PP}^2, R_{QQ}^2 and KS, the non-parametric model KE generally does not provide improved fits compared to parametric models. However, based on χ^2, KE is the best distribution followed closely by MWW/LS. Both pdfs are ranked first at 3 stations each. As χ^2 puts more weight on class intervals with lower frequency, it could be hypothesized that KE models better the upper tail of wind speed distributions than other pdfs.

Figure 6 illustrates the frequency histograms and normal probability plots of the wind speed of each station. The pdfs of W2/MM, KAP/LM, MWW/LS and KE are superimposed over these plots. These D/Ms are selected to represent the one-component parametric, the mixture and the non-parametric models. KAP/LM is selected among one-component parametric distributions because it has been shown to lead to the overall best performances for the 7 stations. The W2 is included for comparison purposes since it is commonly accepted for wind speed modeling. It can be noticed that KAP/LM shows considerably more flexibility for Masdar City and Sir Bani Yas Island. The W2 is generally not suitable. For instance, it overestimates wind speed frequencies for bins of median wind speed for Al Aradh and Sir Bani Yas Island and underestimates them for East of Jebel Haffet and Madinat Zayed. Histograms of Al Aradh, Masdar City and Sir Bani Yas Island show clearly the presence of a bimodal regime. In these cases, the more flexible models MWW/LS and KE show a clear advantage. MWW/LS is the most flexible distribution and it is particularly efficient to model the histograms of Masdar City and Sir Bani Yas Island. For a station presenting a strong unimodal regime, like Al Mirfa, the fits given by the different models are all similar.

4.3 Stations at different heights

Table 6 presents the goodness-of-fit statistics obtained with each D/M at each height for the station of Al Hala and the Masdar Wind Station. The values of the statistics are presented with box plots in Figures 7 and 8 for the station of Al Hala and the Masdar Wind Station respectively. Tables 7 and 8 list the 6 best D/Ms based on every statistic for each station respectively.

Performances of one-component parametric models are first evaluated. Box plots reveal that for Al Hala, very good fits and small variances of the statistics are obtained for the majority of distributions. The small variance indicates a slight variation of the wind speed distribution between the heights of 40 m and 80 m. The W2 is one of the distributions giving the best statistics. For the Masdar Wind Station, the variance of the various statistics is higher. KAP/LM is by far the best D/M for every statistic.

Analysis of Table 7 reveals that, for the Al Hala station, W3/ML followed by GG/ML are the best D/Ms at every height according to ln L. P3/MM is the best D/M at 40 m and 60 m height, and W2/ML is the best D/M at 80 m based on R_{PP}^2. GG/MM followed by GG/ML and W3/ML give the best fits with respect to R_{QQ}^2. GG/ML at 40 m and 60 m, and W3/ML at 80 m give the best fit with respect to χ^2. P3/MM is the best D/M at 40 m and 80 m, and LN3/MM is the best D/M at 60 m based on KS. For the Masdar Wind Station, analysis of Table 8 reveals that KAP generally represents the best parametric distribution. KAP/ML is the best D/M at three heights according to ln L. KAP/LM is the best D/M at every height based on R_{PP}^2 and KS, and at three heights based on χ^2. Based on R_{QQ}^2, KAP/LM is ranked first at the 10 m and 30 m, and KAP/ML is ranked first at the 40 m heights.

Box plots reveal that mixture models give the overall best fits at both stations. MWW/LS is generally better than MGG/LS. The variance of the boxplots of R_{QQ}^2 for MGG is very high for Al Hala. It is caused by a less accurate fit only at 40 m. Mixture models are superior to KE. In the case of Al Hala, the improvement obtained with mixture models is not very high. For Masdar Wind Station, a flexible model, such as a mixture model, is required. KAP is the only one-component parametric distribution which can model the data.

Figures 9 and 10 present frequency histograms and normal probability plots of wind speed for each height at the station of Al Hala and the Masdar Wind Station respectively. The pdfs of W2/MM, KAP/LM, MWW/LS and KE are superimposed in these plots. Histogram shapes show that all the empirical distributions at Al Hala are unimodal and do not change with height. This explains the small variance in statistics. For Al Hala station, each selected D/M gives approximately the same fit for all 3 heights. Relatively little change is observed from one height to another. In that case, flexible models do not provide any advantages. For the Masdar Wind Station, bimodal shapes are observed at lower heights and become unimodal at higher heights. At lower altitudes, the more flexible model MWW/LS and KE clearly show an advantage while at 50 m, all models provide equivalent fits.

5 Conclusions

The W2 distribution has been frequently suggested for the characterization of short term wind speed data in a large number of regions in the world. In this study, 11 one-component pdfs, 2 two-component mixture pdfs and the kernel density pdf were fitted to hourly average wind speed series from 9 meteorological stations located in the UAE. This region is characterized by a severe lack of studies focusing on the assessment of wind speed characteristics and distributions. For each pdf, one or more estimation methods were used to estimate the parameters of the distribution. Different goodness-of-fit measurements have been used to evaluate the suitability of pdfs over wind speed data.

Overall, mixture distributions are generally the best pdfs according to every statistic. MWW is more suitable than MGG most of the time. The non-parametric KE method does not generally lead to best performances. Results show also clearly that one-component pdfs are not suitable for modeling distributions presenting bimodal regimes. In this case, mixture distributions should be employed.

Overall, and for all stations and heights, the best one-component pdfs are KAP and GG. W2 is the best 2-parameter distribution and performs better than some 3-parameter distributions such as the GEV and LN3.

Acknowledgements

The financial support provided by the Masdar Institute of Science and Technology is gratefully acknowledged. The authors wish to thank Masdar Power for having supplied the wind speed data used in this study.

Nomenclature

C_V	coefficient of variation
C_S	coefficient of skewness
C_K	coefficient of kurtosis
cdf	cumulative distribution function
χ^2	Chi-square test statistic
D/M	distribution/method
EV1	Gumbel or extreme value type I distribution
$f_{\hat{\theta}}(\ )$	probability density function with estimated parameters $\hat{\theta}$
$\hat{f}(\ )$	estimated probability density function
F_i	empirical probability for the i^{th} wind speed observation
$\hat{F}_i$	estimated cumulative probability for the i^{th} observation obtained with the theoretical cdf
$F(\ )$	cumulative distribution function
$F^{-1}(\ )$	inverse of a given cumulative distribution function
G	Gamma distribution
GEV	generalized extreme value distribution
GG	generalized Gamma distribution
GMM	generalized method of moment
K( )	kernel function
KAP	Kappa distribution

KE	Kernel density distribution
KS	Kolmogorov-Smirnov test statistic
LN2	2-parameter Lognormal distribution
LN3	3-parameter Lognormal distribution
MGG	mixture of two Gamma pdfs
ML	maximum likelihood
MM	method of moments
MWW	mixture of two 2-parameter Weibull pdfs
n	number of wind speed observations in a series of wind speed observations
N	number of bins in a histogram of wind speed data
P3	Pearson type III distribution
pdf	probability density function
R^2	coefficient of determination
R_{PP}^2	coefficient of determination giving the degree of fit between the theoretical cdf and the empirical cumulative probabilities of wind speed data.
R_{QQ}^2	coefficient of determination giving the degree of fit between the theoretical wind speed quantiles and the wind speed data.
RAY	Rayleigh distribution
rmse	root mean square error
v_i	the i^{th} observation of the wind speed series
$\hat{v}_i$	predicted wind speed for the i^{th} observation

W2	2-parameter Weibull distribution
W3	3-parameter Weibull distribution
WMM	weighted method of moments

References

Acker, T.L., Williams, S.K., Duque, E.P.N., Brummels, G., Buechler, J., 2007. Wind resource assessment in the state of Arizona: Inventory, capacity factor, and cost. Renewable Energy 32(9), 1453-1466.

Ahmed Shata, A.S., Hanitsch, R., 2006. Evaluation of wind energy potential and electricity generation on the coast of Mediterranean Sea in Egypt. Renewable Energy 31(8), 1183-1202.

Akpinar, E.K., Akpinar, S., 2005. A statistical analysis of wind speed data used in installation of wind energy conversion systems. Energy Conversion and Management 46(4), 515-532.

Akpinar, S., Kavak Akpinar, E., 2007. Wind energy analysis based on maximum entropy principle (MEP)-type distribution function. Energy Conversion and Management 48(4), 1140-1149.

Akpinar, S., Akpinar, E.K., 2009. Estimation of wind energy potential using finite mixture distribution models. Energy Conversion and Management 50(4), 877-884.

Algifri, A.H., 1998. Wind energy potential in Aden-Yemen. Renewable Energy 13(2), 255-260.

Archer, C.L., Jacobson, M.Z., 2003. Spatial and temporal distributions of U.S. winds and wind power at 80 m derived from measurements. Journal of Geophysical Research: Atmospheres 108(D9), 4289.

Ashkar, F., Ouarda, T.B.M.J., 1996. On some methods of fitting the generalized Pareto distribution. Journal of Hydrology 177(1–2), 117-141.

Auwera, L., Meyer, F., Malet, L., 1980. The use of the Weibull three-parameter model for estimating mean power densities. Journal of Applied Meteorology 19, 819-825.

Ayodele, T.R., Jimoh, A.A., Munda, J.L., Agee, J.T., 2012. Wind distribution and capacity factor estimation for wind turbines in the coastal region of South Africa. Energy Conversion and Management 64(0), 614-625.

Bobée, B., 1975. The Log Pearson Type 3 distribution and its application in hydrology. Water Resources Research 11(5), 681-689.

Bobée, B., Ashkar, F., 1988. Sundry averages method (SAM) for estimating parameters of the Log-Pearson Type 3 distribution. Research Report No. 251, INRS-ETE, Quebec City, Canada.

Carta, J.A., Ramírez, P., 2007. Use of finite mixture distribution models in the analysis of wind energy in the Canarian Archipelago. Energy Conversion and Management 48(1), 281-291.

Carta, J.A., Ramirez, P., Velazquez, S., 2008. Influence of the level of fit of a density probability function to wind-speed data on the WECS mean power output estimation. Energy Conversion and Management 49(10), 2647-2655.

Carta, J.A., Ramirez, P., Velazquez, S., 2009. A review of wind speed probability distributions used in wind energy analysis Case studies in the Canary Islands. Renewable & Sustainable Energy Reviews 13(5), 933-955.

Celik, A.N., 2003. Energy output estimation for small-scale wind power generators using Weibull-representative wind data. Journal of Wind Engineering and Industrial Aerodynamics 91(5), 693-707.

Celik, A.N., 2004. On the distributional parameters used in assessment of the suitability of wind speed probability density functions. Energy Conversion and Management 45(11-12), 1735-1747.

Chang, T.P., 2011. Estimation of wind energy potential using different probability density functions. Applied Energy 88(5), 1848-1856.

Chellali, F., Khellaf, A., Belouchrani, A., Khanniche, R., 2012. A comparison between wind speed distributions derived from the maximum entropy principle and Weibull distribution. Case of study; six regions of Algeria. Renewable & Sustainable Energy Reviews 16(1), 379-385.

Conradsen, K., Nielsen, L.B., Prahm, L.P., 1984. Review of Weibull Statistics for Estimation of Wind Speed Distributions. Journal of Climate and Applied Meteorology 23(8), 1173-1183.

Cunnane, C., 1978. Unbiased plotting positions — A review. Journal of Hydrology 37(3–4), 205-222.

Dorvlo, A.S.S., 2002. Estimating wind speed distribution. Energy Conversion and Management 43(17), 2311-2318.

Fichaux, N., Ranchin, T., 2003. Evaluating the offshore wind potential. A combined approach using remote sensing and statistical methods. In: Proceedings IGARSS'03 - IEEE International Geoscience and Remote Sensing Symposium, Toulouse, France, Vol. 4, pp. 2703-2705.

Garcia, A., Torres, J.L., Prieto, E., De Francisco, A., 1998. Fitting wind speed distributions: A case study. Solar Energy 62(2), 139-144.

Gökçek, M., Bayülken, A., Bekdemir, Ş., 2007. Investigation of wind characteristics and wind energy potential in Kirklareli, Turkey. Renewable Energy 32(10), 1739-1752.

Guidoum, A.C., 2014. kedd: Kernel estimator and bandwidth selection for density and its derivatives. R package version 1.0.1. URL http://CRAN.R-project.org/package=kedd

Hennessey, J.P., 1977. Some aspects of wind power statistics. Journal of Applied Meteorology 16(2), 119-128.

Hosking, J.R.M., Wallis, J.R., 1997. Regional Frequency Analysis: An Approach Based on L-Moments. Cambridge University Press.

Hosking J.R.M., 1996. Fortran routines for use with the method of L-moments, version 3.04. Research report 20525, IBM Research Division.

Hundecha, Y., St-Hilaire, A., Ouarda, T.B.M.J., El Adlouni, S., Gachon, P., 2008. A Nonstationary Extreme Value Analysis for the Assessment of Changes in Extreme Annual Wind Speed over the Gulf of St. Lawrence, Canada. Journal of Applied Meteorology and Climatology 47(11), 2745-2759.

Irwanto, M., Gomesh, N., Mamat, M.R., Yusoff, Y.M., 2014. Assessment of wind power generation potential in Perlis, Malaysia. Renewable and Sustainable Energy Reviews 38(0), 296-308.

Jaramillo, O.A., Saldaña, R., Miranda, U., 2004. Wind power potential of Baja California Sur, México. Renewable Energy 29(13), 2087-2100.

Jones, M.C., Marron, J.S., Sheather, S.J., 1996. A brief survey of bandwidth selection for density estimation. Journal of the American Statistical Association 91(433), 401-407.

Justus, C.G., Hargraves, W.R., Mikhail, A., Graber, D., 1978. Methods for Estimating Wind Speed Frequency Distributions. Journal of Applied Meteorology 17(3), 350-353.

Justus, C.G., Hargraves, W.R., Yalcin, A., 1976. Nationwide assessment of potential output from wind-powered generators. Journal of Applied Meteorology 15(7), 673-678.

Kose, R., Ozgur, M.A., Erbas, O., Tugcu, A., 2004. The analysis of wind data and wind energy potential in Kutahya, Turkey. Renewable and Sustainable Energy Reviews 8(3), 277-288.

Li, M., Li, X., 2005. MEP-type distribution function: a better alternative to Weibull function for wind speed distributions. Renewable Energy 30(8), 1221-1240.

Lo Brano, V., Orioli, A., Ciulla, G., Culotta, S., 2011. Quality of wind speed fitting distributions for the urban area of Palermo, Italy. Renewable Energy 36(3), 1026-1039.

Masseran, N., Razali, A.M., Ibrahim, K., 2012. An analysis of wind power density derived from several wind speed density functions: The regional assessment on wind power in Malaysia. Renewable & Sustainable Energy Reviews 16(8), 6476-6487.

Mirhosseini, M., Sharifi, F., Sedaghat, A., 2011. Assessing the wind energy potential locations in province of Semnan in Iran. Renewable and Sustainable Energy Reviews 15(1), 449-459.

Morgan, E.C., Lackner, M., Vogel, R.M., Baise, L.G., 2011. Probability distributions for offshore wind speeds. Energy Conversion and Management 52(1), 15-26.

Nfaoui, H., Buret, J., Sayigh, A.A.M., 1998. Wind characteristics and wind energy potential in Morocco. Solar Energy 63(1), 51-60.

Ordóñez, G., Osma, G., Vergara, P., Rey, J., 2014. Wind and Solar Energy Potential Assessment for Development of Renewables Energies Applications in Bucaramanga, Colombia. IOP Conference Series: Materials Science and Engineering 59(1), 012004.

Ouarda, T.B.M.J., Charron, C., Niranjan Kumar, K., Marpu, P.R., Ghedira, H., Molini, A., Khayal, I., 2014. Evolution of the rainfall regime in the United Arab Emirates. Journal of Hydrology 514(0), 258-270.

Persaud, S., Flynn, D., Fox, B., 1999. Potential for wind generation on the Guyana coastlands. Renewable Energy 18(2), 175-189.

Petković, D., Shamshirband, S., Anuar, N.B., Saboohi, H., Abdul Wahab, A.W., Protić, M., Zalnezhad, E., Mirhashemi, S.M.A., 2014. An appraisal of wind speed distribution prediction by soft computing methodologies: A comparative study. Energy Conversion and Management 84(0), 133-139.

Poje, D., Cividini, B., 1988. Assessment of wind energy potential in croatia. Solar Energy 41(6), 543-554.

Qin, Z.L., Li, W.Y., Xiong, X.F., 2011. Estimating wind speed probability distribution using kernel density method. Electric Power Systems Research 81(12), 2139-2146.

Qin, X., Zhang, J.-s., Yan, X.-d., 2012. Two Improved Mixture Weibull Models for the Analysis of Wind Speed Data. Journal of Applied Meteorology and Climatology 51(7), 1321-1332.

Ramirez, P., Carta, J.A., 2006. The use of wind probability distributions derived from the maximum entropy principle in the analysis of wind energy. A case study. Energy Conversion and Management 47(15-16), 2564-2577.

Şahin, A.Z., Aksakal, A., 1998. Wind power energy potential at the northeastern region of Saudi Arabia. Renewable Energy 14(1–4), 435-440.

Seguro, J.V., Lambert, T.W., 2000. Modern estimation of the parameters of the Weibull wind speed distribution for wind energy analysis. Journal of Wind Engineering and Industrial Aerodynamics 85(1), 75-84.

Singh, V., Deng, Z., 2003. Entropy-Based Parameter Estimation for Kappa Distribution. Journal of Hydrologic Engineering 8(2), 81-92.

Soukissian, T., 2013. Use of multi-parameter distributions for offshore wind speed modeling: The Johnson SB distribution. Applied Energy 111(0), 982-1000.

Stewart, D.A., Essenwanger, O.M., 1978. Frequency Distribution of Wind Speed Near the Surface. Journal of Applied Meteorology 17(11), 1633-1642.

Sulaiman, M.Y., Akaak, A.M., Wahab, M.A., Zakaria, A., Sulaiman, Z.A., Suradi, J., 2002. Wind characteristics of Oman. Energy 27(1), 35-46.

Takle, E.S., Brown, J.M., 1978. Note on use of Weibull statistics to characterize wind speed data. Journal of Applied Meteorology 17(4), 556-559.

Tuller, S.E., Brett, A.C., 1985. The goodness of fit of the Weilbull and Rayleigh distribution to the distributions of observed wind speeds in a topographically diverse area. Journal of climatology 5, 74-94.

Ulgen, K., Hepbasli, A., 2002. Determination of Weibull parameters for wind energy analysis of Izmir, Turkey. International Journal of Energy Research 26(6), 495-506.

Usta, I., Kantar, Y.M., 2012. Analysis of some flexible families of distributions for estimation of wind speed distributions. Applied Energy 89(1), 355-367.

Water Resources Council, Hydrology Committee, 1967. A uniform technique for determining flood flow frequencies. US Water Resour. Counc., Bull. No. 15, Washington, D.C.

Zhang, H., Yu, Y.-J., Liu, Z.-Y., 2014. Study on the Maximum Entropy Principle applied to the annual wind speed probability distribution: A case study for observations of intertidal zone anemometer towers of Rudong in East China Sea. Applied Energy 114(0), 931-938.

Zhang, J., Chowdhury, S., Messac, A., Castillo, L., 2013. A Multivariate and Multimodal Wind Distribution model. Renewable Energy 51(0), 436-447.

Zhou, J.Y., Erdem, E., Li, G., Shi, J., 2010. Comprehensive evaluation of wind speed distribution models: A case study for North Dakota sites. Energy Conversion and Management 51(7), 1449-1458.

Table 1. Description of the meteorological stations.

Station	Measuring Height (m)	Altitude (m)	Latitude	Longitude	Period (year/month)
Al Aradh	10	178	23.903° N	55.499° E	2007/06 - 2010/08
Al Mirfa	10	6	24.122° N	53.443° E	2007/06 - 2009/07
Al Wagan	10	142	23.579° N	55.419° E	2009/08 - 2010/08
East of Jebel Haffet	10	341	24.168° N	55.864° E	2009/10 - 2010/08
Madinat Zayed	10	137	23.561° N	53.709° E	2008/06 - 2010/08
Masdar City	10	7	24.420° N	54.613° E	2008/07 - 2010/08
Sir Bani Yas Island	10	7	24.322° N	52.566° E	2007/06 - 2010/08
Al Hala	40, 60, 80	N/A	25.497° N	56.143° E	2009/08 - 2010/08
Masdar Wind Station	10, 30, 40, 50	0.6	24.420° N	54.613° E	2008/08 - 2011/02

Table 2. List of probability density functions, domain, number of parameters and estimation methods used.

Name	pdf	Domain	Number of parameters	Estimation method
EV1	$f(x)=\frac{1}{\alpha}\exp\left[-\frac{x-\mu}{\alpha}-\exp\left(\frac{x-\mu}{\alpha}\right)\right]$	$-\infty<x<+\infty$	2	ML, MM
W2	$f(x)=\frac{k}{\alpha}\left(\frac{x}{\alpha}\right)^{k-1}\exp\left[-\left(\frac{x}{\alpha}\right)^{k}\right]$	$x>0$	2	ML, MM
G	$f(x)=\frac{\alpha^{k}}{\Gamma(k)}x^{k-1}\exp(-\alpha x)$	$x>0$	2	ML, MM
LN2	$f(x)=\frac{1}{x\alpha\sqrt{2\pi}}\exp\left[-\frac{(\ln x-\mu)^{2}}{2\alpha^{2}}\right]$	$x>0$	2	ML, MM
W3	$f(x)=\frac{k}{\alpha}\left(\frac{x-\mu}{\alpha}\right)^{k-1}\exp\left[-\left(\frac{x-\mu}{\alpha}\right)^{k}\right]$	$x>\mu$	3	ML
LN3	$f(x)=\frac{1}{(x-m)\alpha\sqrt{2\pi}}\exp\left\{-\frac{\left[\ln(x-m)-\mu\right]^{2}}{2\alpha^{2}}\right\}$	$x>m$	3	ML, MM
GEV	$f(x)=\frac{1}{\alpha}\left[1-\frac{k}{\alpha}(x-u)\right]^{\frac{1}{k}-1}\exp\left\{-\left[1-\frac{k}{\alpha}(x-u)\right]^{1/k}\right\}$	$x>u+\alpha/k$ if $k<0$ $x<u+\alpha/k$ if $k>0$	3	ML, MM
GG	$f(x)=\frac{\lvert h\rvert\alpha^{hk}}{\Gamma(k)}x^{hk-1}\exp(-\alpha x)^{h}$	$x>0$	3	ML, MM
P3	$f(x)=\frac{\alpha^{k}}{\Gamma(k)}(x-\mu)^{k-1}\exp\left[-\alpha(x-\mu)\right]$	$x>\mu$	3	ML, MM
LP3	$f(x)=\frac{g\lvert\alpha\rvert}{x\Gamma(k)}\left[\alpha(\log_{a}x-\mu)\right]^{k-1}\exp\left[-\alpha(\log_{a}x-\mu)\right]$ $g=\log_{a}e$	$x>e^{\mu/g}$ if $\alpha>0$ $0<x<e^{\mu/g}$ if $\alpha<0$	3	GMM
KAP	$f(x)=\alpha^{-1}[1-k(x-\mu)/\alpha]^{1/k-1}[F(x)]^{1-h}$ where $F(x)=(1-h(1-k(x-\mu)/\alpha)^{1/k})^{1/h}$	$x\le\mu+\alpha/k$ if $k>0$ $\mu+\alpha(1-h^{-k})/k\le x$ if $k>0$ $\mu+\alpha/k\le x$ if $h\le 0, k<0$	4	LM, ML
MWW	$f(x)=\omega\frac{k_1}{\alpha_1}\left(\frac{x}{\alpha_1}\right)^{k_1-1}\exp\left[-\left(\frac{x}{\alpha_1}\right)^{k_1}\right]+(1-\omega)\frac{k_2}{\alpha_2}\left(\frac{x}{\alpha_2}\right)^{k_2-1}\exp\left[-\left(\frac{x}{\alpha_2}\right)^{k_2}\right]$	$x>0$	5	LS
MGG	$f(x)=\omega\frac{\alpha^{k_1}}{\Gamma(k_1)}x^{k_1-1}\exp(-\alpha_1 x)+(1-\omega)\frac{\alpha_2^{k_2}}{\Gamma(k_2)}x^{k_2-1}\exp(-\alpha_2 x)$	$x>0$	5	LS

μ: location parameter.
m: second location parameter (LN3).
α: scale parameter.
k: shape parameter.
h: second shape parameter (GG, KAP).
ω: mixture parameter (MWW, MGG).
$\Gamma(\,)$: gamma function.

Table 3. Descriptive statistics of wind speed series. Maximum, mean, median, standard deviation (SD), coefficient of variation (C_V), coefficient of skewness (C_S) and coefficient of kurtosis (C_K).

Station	Height (m)	Maximum (m/s)	Mean (m/s)	Median (m/s)	SD (m/s)	C_V	C_S	C_K
Al Aradh	10	12.42	2.47	2.20	1.73	0.70	0.97	4.20
Al Mirfa	10	17.17	4.28	3.96	2.26	0.53	0.71	3.58
Al Wagan	10	12.36	3.67	3.31	2.22	0.61	0.66	3.08
East of Jebel Haffet	10	16.41	4.27	3.87	2.35	0.55	0.99	4.47
Madinat Zayed	10	18.04	4.10	3.56	2.44	0.60	0.94	3.83
Masdar City	10	12.17	3.09	2.67	2.06	0.67	0.70	2.90
Sir Bani Yas Island	10	13.95	3.86	3.76	2.14	0.55	0.43	3.06
Al Hala	40	16.42	5.61	5.43	2.66	0.47	0.58	3.29
	60	16.72	5.67	5.50	2.72	0.48	0.56	3.27
	80	16.67	5.80	5.63	2.68	0.46	0.54	3.25
Masdar Wind Station	10	13.02	3.16	2.69	1.87	0.59	0.82	3.09
	30	15.20	3.85	3.44	2.01	0.52	0.80	3.37
	40	15.73	4.06	3.71	2.02	0.50	0.76	3.43
	50	16.26	4.37	4.05	2.13	0.49	0.77	3.73

Table 4. Statistics obtained with each D/M for the stations at 10 m height.

Statistic	D/M	Al Aradh	Al Mirfa	Al Wagan	East of Jebel Haffet	Madinat Zayed	Masdar City	Sir Bani Yas Island
ln *L*								
	EV1/ML	-51761	-40610	-13777	-14608	-39966	-37939	-58656
	EV1/MM	-51763	-40685	-13789	-14610	-39968	-37943	-59097
	W2/ML	-50928	-40561	-13664	-14664	-40032	-37156	-58726
	W2/MM	-51070	-40564	-13670	-14664	-40034	-37172	-58873
	W3/ML	-50717	**-40468**	-13622	-14654	-39916	-37130	-57870
	LN2/ML	-57510	-43750	-14901	-15502	-43435	-39738	-67410
	LN2/MM	-74925	-47170	-16939	-16309	-47573	-44668	-87395
	G/ML	-51519	-41044	-13841	-14745	-40339	-37452	-60260
	G/MM	-52696	-41280	-13995	-14781	-40502	-37767	-62402
	GEV/ML	-51730	-40551	-13773	-14608	-39954	-37914	-58239
	GEV/MM	-51854	-40561	-13794	-14610	-40038	-38121	-58246
	LN3/ML	-51537	-40538	-13752	-14605	-39911	-37709	-58250
	LN3/MM	-51813	-40573	-13810	-14608	-40041	-38185	-58278
	GG/ML	-50349	-40554	**-13608**	-14658	-40032	-37017	-57778
	GG/MM	-50556	-40596	-13610	-14709	-40081	-37031	-57902
	P3/ML	-51084	-40492	-13694	-14605	-39861	-37340	-58196
	P3/MM	-51535	-40523	-13783	-14615	-39923	-38073	-58249
	LP3/GMM	x	x	-13706	-14831	-40493	x	x
	KAP/ML	-50738	-40477	-13614	**-14603**	**-39847**	-36999	-58063
	KAP/LM	-51251	-40491	-13623	-14604	-39905	x	x
	MWW/LS	-50520	-40570	-13633	-14616	-40263	**-36979**	**-57288**
	MGG/LS	**-50228**	-40921	-13702	-14772	-40587	-37182	-58114
	KE	-51754	-40623	-13815	-14697	-40027	-37544	-58080
R_{PP}^2								
	EV1/ML	0.9972	0.9986	0.9958	0.9998	0.9977	0.9871	0.9917
	EV1/MM	0.9976	0.9962	0.9926	0.9997	0.9975	0.9855	0.9858
	W2/ML	0.9922	0.9994	0.9984	0.9962	0.9962	0.9960	0.9869
	W2/MM	0.9970	0.9996	0.9985	0.9963	0.9962	0.9943	0.9947
	W3/ML	0.9968	0.9994	0.9990	0.9960	0.9956	0.9957	0.9980
	LN2/ML	0.9167	0.9640	0.9538	0.9707	0.9619	0.9709	0.8844
	LN2/MM	0.9636	0.9843	0.9695	0.9930	0.9911	0.9526	0.9600
	G/ML	0.9793	0.9939	0.9908	0.9956	0.9957	0.9936	0.9594
	G/MM	0.9919	0.9975	0.9927	0.9994	0.9991	0.9872	0.9841
	GEV/ML	0.9967	0.9990	0.9956	0.9997	0.9985	0.9885	0.9984
	GEV/MM	0.9984	0.9991	0.9961	0.9995	0.9964	0.9877	0.9989
	LN3/ML	0.9964	0.9991	0.9963	0.9997	0.9989	0.9909	0.9982
	LN3/MM	0.9986	0.9989	0.9955	0.9994	0.9961	0.9868	0.9991
	GG/ML	0.9965	0.9992	0.9992	0.9973	0.9960	0.9966	0.9935
	GG/MM	0.9985	0.9998	0.9993	0.9992	0.9977	0.9971	0.9981
	P3/ML	0.9942	0.9995	0.9973	0.9993	0.9986	0.9943	0.9977
	P3/MM	0.9993	0.9994	0.9964	0.9994	0.9973	0.9885	0.9991
	LP3/GMM	0.9961	0.9995	0.9995	0.9989	0.9984	0.9988	0.9954
	KAP/ML	0.9938	0.9998	0.9995	0.9996	0.9984	0.9982	0.9960
	KAP/LM	0.9994	**0.9998**	0.9996	0.9997	0.9989	0.9992	0.9993
	MWW/LS	**0.9994**	0.9997	**0.9998**	**0.9999**	**0.9993**	**0.9999**	**0.9999**
	MGG/LS	0.9999	0.9997	0.9992	0.9997	0.9992	0.9991	0.9996
	KE	0.9988	0.9988	0.9973	0.9963	0.9978	0.9978	0.9993
R_{QQ}^2								
	EV1/ML	0.9943	0.9867	0.9813	0.9975	0.9930	0.9750	0.9569
	EV1/MM	0.9945	0.9907	0.9833	0.9978	0.9931	0.9753	0.9746
	W2/ML	0.9880	0.9990	0.9944	0.9936	0.9972	0.9854	0.9827
	W2/MM	0.9974	0.9991	0.9966	0.9935	0.9971	0.9886	0.9936

W3/ML	0.9963	0.9988	0.9973	0.9927	0.9964	0.9874	0.9979
LN2/ML	-5.2432	0.3112	-0.6784	0.5905	-0.0827	-0.5727	-4.1144
LN2/MM	0.9414	0.9621	0.9319	0.9778	0.9616	0.9079	0.9259
G/ML	0.9346	0.9761	0.9468	0.9915	0.9834	0.9433	0.8618
G/MM	0.9907	0.9937	0.9832	0.9979	0.9950	0.9733	0.9754
GEV/ML	0.9874	0.9982	0.9893	0.9984	0.9882	0.9506	0.9965
GEV/MM	0.9955	0.9987	0.9940	0.9987	0.9949	0.9844	0.9966
LN3/ML	0.9825	0.9971	0.9819	0.9983	0.9896	0.9314	0.9956
LN3/MM	0.9958	0.9984	0.9927	0.9985	0.9946	0.9829	0.9962
GG/ML	0.9961	0.9985	0.9992	0.9957	0.9970	0.9966	0.9937
GG/MM	0.9985	0.9994	**0.9992**	0.9982	0.9979	0.9973	0.9974
P3/ML	0.9847	0.9986	0.9862	0.9984	0.9967	0.9621	0.9956
P3/MM	0.9980	0.9992	0.9944	0.9986	0.9968	0.9858	0.9966
LP3/GMM	0.9954	0.9981	0.9984	0.9977	**0.9985**	0.9973	0.9919
KAP/ML	0.9930	0.9992	0.9988	**0.9989**	0.9982	0.9962	0.9951
KAP/LM	0.9983	0.9990	0.9988	0.9988	0.9978	0.9967	0.9969
MWW/LS	0.9946	**0.9994**	0.9987	0.9970	0.9954	**0.9979**	**0.9992**
MGG/LS	**0.9990**	0.9990	0.9944	0.9977	0.9950	0.9917	0.9969
KE	0.9957	0.9965	0.9909	0.9919	0.9956	0.9944	0.9971
χ^2							
EV1/ML	809.9	281.8	218.1	54.3	315.3	1366.2	1484.3
EV1/MM	800.6	509.3	302.0	64.8	300.8	1441.4	2763.9
W2/ML	470.7	98.1	69.8	188.9	335.9	576.9	1003.5
W2/MM	216.1	94.6	70.9	190.6	327.3	596.0	869.9
W3/ML	229.2	115.4	58.0	211.0	358.0	566.1	430.4
LN2/ML	6478.1	2303.7	890.0	604.7	2083.3	2493.3	9277.9
LN2/MM	3474.9	8722.8	2392.6	1990.3	4107.4	5099.5	22218.7
G/ML	1301.3	467.4	220.7	127.3	376.2	896.4	2864.7
G/MM	575.3	609.2	317.0	127.0	302.2	1154.1	3444.6
GEV/ML	785.4	146.5	205.9	53.9	312.0	1400.6	749.4
GEV/MM	764.9	116.3	169.0	**52.2**	293.4	1222.2	705.0
LN3/ML	629.5	148.8	192.0	54.2	268.4	1231.3	784.5
LN3/MM	705.5	120.1	178.7	54.5	310.2	1281.2	697.3
GG/ML	411.1	132.5	43.3	134.8	355.7	362.6	542.6
GG/MM	161.5	80.1	38.2	93.7	242.4	354.5	339.5
P3/ML	453.6	105.0	137.1	67.5	215.3	834.5	763.0
P3/MM	457.7	89.6	148.3	70.2	246.2	1119.7	660.5
LP3/GMM	414.0	197.2	62.7	136.4	218.0	262.0	1740.0
KAP/ML	476.4	85.5	43.4	56.8	194.5	321.6	658.8
KAP/LM	320.1	97.8	56.6	54.8	203.9	454.0	669.6
MWW/LS	176.2	77.1	**12.7**	86.0	783.7	191.8	**101.2**
MGG/LS	**73.0**	164.6	57.8	123.0	289.8	292.7	192.8
KE	316.7	**64.5**	55.2	71.2	**93.9**	**168.6**	151.2
KS							
EV1/ML	0.029	0.023	0.039	0.011	0.025	0.054	0.045
EV1/MM	0.030	0.032	0.044	0.013	0.026	0.056	0.052
W2/ML	0.045	0.017	0.026	0.034	0.031	0.039	0.059
W2/MM	0.031	0.012	0.025	0.033	0.030	0.040	0.034
W3/ML	0.030	0.014	0.023	0.033	0.034	0.038	0.024
LN2/ML	0.134	0.083	0.093	0.081	0.093	0.075	0.155
LN2/MM	0.107	0.056	0.081	0.046	0.051	0.099	0.093
G/ML	0.071	0.033	0.041	0.037	0.039	0.046	0.099
G/MM	0.052	0.026	0.044	0.018	0.018	0.054	0.056
GEV/ML	0.029	0.018	0.036	0.012	0.024	0.055	0.022
GEV/MM	0.037	0.016	0.034	0.013	0.033	0.058	0.020
LN3/ML	0.029	0.017	0.036	0.011	0.020	0.053	0.023
LN3/MM	0.037	0.018	0.036	0.015	0.035	0.060	0.021
GG/ML	0.032	0.019	0.018	0.030	0.032	0.032	0.044

GG/MM	0.020	0.009	0.015	0.017	0.024	0.028	0.024
P3/ML	0.040	0.014	0.033	0.016	0.021	0.046	0.022
P3/MM	0.032	0.014	0.032	0.014	0.029	0.056	0.021
LP3/GMM	0.033	0.013	0.014	0.019	0.021	0.018	0.035
KAP/ML	0.041	0.009	0.015	0.012	0.022	0.026	0.034
KAP/LM	0.024	**0.007**	0.012	**0.010**	0.016	0.019	0.019
MWW/LS	0.018	0.009	**0.012**	0.010	**0.014**	**0.006**	**0.006**
MGG/LS	**0.009**	0.014	0.017	0.018	0.016	0.016	0.013
KE	0.047	0.020	0.035	0.036	0.026	0.037	0.024

x The ln *L* statistic cannot be calculated for this series.
Best statistics are in bold characters.

Table 5. Ranking of D/Ms for all stations at the 10 m height based on the goodness-of-fit statistics.

Statistic	Station	Rank of D/M					
		1st	2nd	3rd	4th	5th	6th
ln L							
	Al Aradh	MGG/LS[b]	GG/ML[a]	MWW/LS	GG/MM	W3/ML	KAP/ML
	Al Mirfa	W3/ML[a]	KAP/ML	KAP/LM	P3/ML	P3/MM	LN3/ML
	Al Wagan	GG/ML[a]	GG/MM	KAP/ML	W3/ML	KAP/LM	MWW/LS[b]
	East of Jebel Haffet	KAP/ML[a]	KAP/LM	LN3/ML	P3/ML	LN3/MM	GEV/ML
	Madinat Zayed	KAP/ML[a]	P3/ML	KAP/LM	LN3/ML	W3/ML	P3/MM
	Masdar City	MWW/LS[b]	KAP/ML[a]	GG/ML	GG/MM	W3/ML	Wb/ML
	Sir Bani Yas Island	MWW/LS[b]	GG/ML[a]	W3/ML	GG/MM	KAP/ML	KE
R_{PP}^2							
	Al Aradh	MGG/LS[b]	KAP/LM[a]	MWW/LS	P3/MM	KE	LN3/MM
	Al Mirfa	KAP/LM[a]	KAP/ML	GG/MM	MGG/LS[b]	MWW/LS	Wb/MM
	Al Wagan	MWW/LS[b]	KAP/LM[a]	LP3/GMM	KAP/ML	GG/MM	GG/ML
	East of Jebel Haffet	MWW/LS[b]	EVa/ML[a]	KAP/LM	GEV/ML	MGG/LS	EVa/MM
	Madinat Zayed	MWW/LS[b]	MGG/LS	G/MM[a]	LN3/ML	KAP/LM	P3/ML
	Masdar City	MWW/LS[b]	KAP/LM[a]	MGG/LS	LP3/GMM	KAP/ML	KE
	Sir Bani Yas Island	MWW/LS[b]	MGG/LS	KE	KAP/LM[a]	P3/MM	LN3/MM
R_{QQ}^2							
	Al Aradh	MGG/LS[b]	GG/MM[a]	KAP/LM	P3/MM	Wb/MM	W3/ML
	Al Mirfa	MWW/LS[b]	GG/MM[a]	KAP/ML	P3/MM	Wb/MM	MGG/LS
	Al Wagan	GG/MM[a]	GG/ML	KAP/LM	KAP/ML	MWW/LS	LP3/GMM
	East of Jebel Haffet	KAP/ML[a]	KAP/LM	GEV/MM	P3/MM	LN3/MM	P3/ML
	Madinat Zayed	LP3/GMM[a]	KAP/ML	GG/MM	KAP/LM	Wb/ML	Wb/MM
	Masdar City	MWW/LS[b]	GG/MM[a]	LP3/GMM	KAP/LM	GG/ML	KAP/ML
	Sir Bani Yas Island	MWW/LS[b]	W3/ML[a]	GG/MM	KE	KAP/LM	MGG/LS
χ^2							
	Al Aradh	MGG/LS[b]	GG/MM[a]	MWW/LS	Wb/MM	W3/ML	KE
	Al Mirfa	KE	MWW/LS[b]	GG/MM[a]	KAP/ML	P3/MM	Wb/MM
	Al Wagan	MWW/LS[b]	GG/MM[a]	GG/ML	KAP/ML	KE	KAP/LM
	East of Jebel Haffet	GEV/MM[a]	GEV/ML	LN3/ML	EVa/ML	LN3/MM	KAP/LM
	Madinat Zayed	KE	KAP/ML[a]	KAP/LM	P3/ML	LP3/GMM	GG/MM
	Masdar City	KE	MWW/LS[b]	LP3/GMM[a]	MGG/LS	KAP/ML	GG/MM
	Sir Bani Yas Island	MWW/LS[b]	KE	MGG/LS	GG/MM[a]	W3/ML	GG/ML
KS							
	Al Aradh	MGG/LS[b]	MWW/LS	GG/MM[a]	KAP/LM	LN3/ML	EVa/ML
	Al Mirfa	KAP/LM[a]	MWW/LS[b]	KAP/ML	GG/MM	Wb/MM	LP3/GMM
	Al Wagan	MWW/LS[b]	KAP/LM[a]	LP3/GMM	KAP/ML	GG/MM	MGG/LS
	East of Jebel Haffet	KAP/LM[a]	MWW/LS[b]	LN3/ML	EVa/ML	KAP/ML	GEV/ML
	Madinat Zayed	MWW/LS[b]	MGG/LS	KAP/LM[a]	G/MM	LN3/ML	P3/ML
	Masdar City	MWW/LS[b]	MGG/LS	LP3/GMM[a]	KAP/LM	KAP/ML	GG/MM
	Sir Bani Yas Island	MWW/LS[b]	MGG/LS	KAP/LM[a]	GEV/MM	P3/MM	LN3/MM

[a]best one-component parametric pdf
[b]best mixture parametric pdf

Table 6. Statistics obtained with each D/M at different heights of Al Hala and Masdar Wind Station.

Statistic	D/M	Al Hala			Masdar Wind Station			
		40 m	60 m	80 m	10 m	30 m	40 m	50 m
ln L								
	EV1/ML	-20346	-20568	-20487	-35315	-37082	-37467	-38357
	EV1/MM	-20426	-20658	-20585	-35329	-37144	-37532	-38389
	W2/ML	-20216	-20418	-20338	-35022	-37083	-37467	-38365
	W2/MM	-20216	-20418	-20338	-35033	-37067	-37458	-38366
	W3/ML	-20207	-20416	-20327	-34933	-36939	-37303	-38298
	LN2/ML	-20820	-21125	-20929	-34983	-37317	-37830	-38789
	LN2/MM	-21304	-21712	-21383	-35480	-37605	-38151	-39270
	G/ML	-20326	-20566	-20455	-34785	-36881	-37311	-38226
	G/MM	-20366	-20619	-20495	-34785	-36926	-37353	-38238
	GEV/ML	-20272	-20485	-20396	-35152	-37093	-37471	-38342
	GEV/MM	-20274	-20486	-20397	-35548	-37191	-37525	-38368
	LN3/ML	-20272	-20485	-20396	-34901	-37005	-37417	-38302
	LN3/MM	-20283	-20494	-20405	-35589	-37220	-37541	-38373
	GG/ML	-20209	-20417	-20332	-34767	-36758	-37153	-38197
	GG/MM	-20209	-20418	-20332	-35035	-36908	-37304	-38202
	P3/ML	-20252	-20466	-20378	-34752	-36758	-37168	-38220
	P3/MM	-20268	-20480	-20392	-35423	-37092	-37435	-38292
	LP3/GMM	-20234	-20456	-20356	-34776	-36829	-37266	-38188
	KAP/ML	-20228	-20443	-20354	-34714	-36723	-37129	-38196
	KAP/LM	-20261	-20477	-20389	x	x	x	x
	MWW/LS	**-20200**	**-20397**	**-20319**	**-34205**	**-36620**	-37126	-38257
	MGG/LS	-20215	-20415	-20344	-34498	-36636	**-37098**	**-38157**
	KE	-20319	-20529	-20435	-34820	-36920	-37346	-38398
R_{PP}^2								
	EV1/ML	0.9952	0.9947	0.9942	0.9810	0.9786	0.9825	0.9977
	EV1/MM	0.9916	0.9910	0.9900	0.9828	0.9732	0.9775	0.9956
	W2/ML	0.9994	0.9993	0.9994	0.9870	0.9704	0.9711	0.9982
	W2/MM	0.9994	0.9993	0.9994	0.9900	0.9735	0.9733	0.9985
	W3/ML	0.9993	0.9992	0.9992	0.9881	0.9945	0.9970	0.9988
	LN2/ML	0.9761	0.9725	0.9755	0.9914	0.9926	0.9933	0.9907
	LN2/MM	0.9810	0.9794	0.9801	0.9706	0.9869	0.9880	0.9874
	G/ML	0.9935	0.9921	0.9928	0.9898	0.9825	0.9849	0.9988
	G/MM	0.9949	0.9941	0.9942	0.9893	0.9789	0.9813	0.9983
	GEV/ML	0.9989	0.9989	0.9987	0.9870	0.9771	0.9791	0.9979
	GEV/MM	0.9992	0.9992	0.9991	0.9826	0.9719	0.9751	0.9985
	LN3/ML	0.9987	0.9987	0.9986	0.9905	0.9799	0.9810	0.9982
	LN3/MM	0.9994	0.9994	0.9993	0.9820	0.9708	0.9740	0.9984
	GG/ML	0.9993	0.9992	0.9992	0.9909	0.9975	0.9989	0.9995
	GG/MM	0.9993	0.9992	0.9992	0.9899	0.9775	0.9792	0.9996
	P3/ML	0.9986	0.9985	0.9984	0.9907	0.9977	0.9989	0.9990
	P3/MM	0.9995	0.9994	0.9993	0.9848	0.9737	0.9764	0.9991
	LP3/GMM	0.9984	0.9981	0.9982	0.9930	0.9804	0.9815	0.9997
	KAP/ML	0.9984	0.9982	0.9981	0.9902	0.9978	0.9994	0.9996
	KAP/LM	0.9994	0.9994	0.9993	0.9983	0.9994	0.9998	0.9999
	MWW/LS	0.9999	**0.9999**	**0.9999**	**0.9998**	**1.0000**	0.9999	0.9999
	MGG/LS	**0.9999**	0.9996	0.9993	0.9980	0.9997	**1.0000**	**1.0000**
	KE	0.9983	0.9983	0.9983	0.9961	0.9981	0.9986	0.9989
R_{QQ}^2								
	EV1/ML	0.9745	0.9725	0.9704	0.9758	0.9761	0.9659	0.9904
	EV1/MM	0.9842	0.9834	0.9824	0.9765	0.9772	0.9719	0.9921
	W2/ML	0.9984	0.9987	0.9985	0.9903	0.9810	0.9769	0.9959

W2/MM	0.9984	0.9987	0.9985	0.9912	0.9826	0.9781	0.9962
W3/ML	0.9987	0.9988	0.9988	0.9909	0.9953	0.9967	0.9971
LN2/ML	0.8107	0.7723	0.8228	0.8421	0.8790	0.8528	0.9047
LN2/MM	0.9631	0.9605	0.9629	0.9404	0.9656	0.9700	0.9752
G/ML	0.9845	0.9811	0.9838	0.9831	0.9828	0.9754	0.9961
G/MM	0.9920	0.9910	0.9915	0.9833	0.9839	0.9787	0.9973
GEV/ML	0.9981	0.9982	0.9981	0.8809	0.9800	0.9774	0.9962
GEV/MM	0.9983	0.9983	0.9982	0.9809	0.9823	0.9786	0.9977
LN3/ML	0.9967	0.9970	0.9970	0.9156	0.9755	0.9725	0.9942
LN3/MM	0.9977	0.9978	0.9977	0.9800	0.9813	0.9780	0.9976
GG/ML	0.9989	0.9989	0.9989	0.9732	0.9945	0.9979	0.9992
GG/MM	0.9989	0.9989	0.9989	0.9912	0.9859	0.9812	0.9993
P3/ML	0.9973	0.9975	0.9974	0.9820	0.9933	0.9954	0.9973
P3/MM	0.9982	0.9983	0.9982	0.9841	0.9835	0.9797	0.9987
LP3/GMM	0.9979	0.9974	0.9977	0.9941	0.9872	0.9818	0.9990
KAP/ML	0.9981	0.9979	0.9978	0.9903	0.9976	0.9991	0.9988
KAP/LM	0.9985	0.9984	0.9983	0.9969	0.9986	0.9990	0.9980
MWW/LS	**0.9995**	**0.9997**	**0.9996**	**0.9997**	0.9995	**0.9991**	0.9971
MGG/LS	0.9933	0.9982	0.9974	0.9974	**0.9995**	0.9990	**0.9998**
KE	0.9940	0.9941	0.9941	0.9936	0.9954	0.9960	0.9962
χ^2							
EV1/ML	233.5	242.2	264.9	1609.9	803.8	603.7	312.3
EV1/MM	483.5	532.5	565.7	1551.4	969.6	795.7	408.2
W2/ML	75.2	63.0	80.5	1298.6	874.0	686.8	345.8
W2/MM	75.2	63.0	80.4	1276.9	830.1	662.7	344.8
W3/ML	67.9	61.7	68.4	1201.5	530.8	328.8	248.6
LN2/ML	1171.8	1231.7	1145.1	1294.6	982.5	1061.3	955.3
LN2/MM	1774.9	2017.1	2106.9	2187.3	1862.6	2346.9	2877.4
G/ML	272.4	304.3	276.0	1043.6	518.9	406.7	143.0
G/MM	423.0	510.3	424.1	1049.2	618.5	507.9	167.1
GEV/ML	107.0	106.4	123.8	1514.1	826.5	626.6	270.8
GEV/MM	98.7	99.0	115.0	1663.0	937.0	688.8	255.8
LN3/ML	108.3	106.8	122.4	1231.1	702.3	552.8	235.5
LN3/MM	96.4	94.8	113.8	1720.3	980.8	710.9	258.1
GG/ML	65.9	60.9	69.8	1035.3	282.0	124.1	89.7
GG/MM	66.6	62.2	70.0	1279.7	583.4	419.6	93.2
P3/ML	101.3	100.2	114.5	1004.2	280.0	150.9	131.6
P3/MM	87.7	86.6	105.6	1546.7	814.5	579.4	180.6
LP3/GMM	127.6	137.6	128.0	940.6	443.8	353.0	68.7
KAP/ML	102.5	99.5	112.0	936.0	219.5	79.6	81.2
KAP/LM	89.3	87.7	107.4	422.6	199.1	**67.6**	119.1
MWW/LS	**33.7**	**24.4**	**38.0**	**36.7**	**48.6**	80.4	213.9
MGG/LS	45.9	36.0	73.6	503.7	70.6	**30.5**	**17.1**
KE	92.9	84.3	108.9	536.5	286.9	232.9	224.9
KS							
EV1/ML	0.0387	0.0403	0.0408	0.0666	0.0740	0.0595	0.0260
EV1/MM	0.0437	0.0454	0.0482	0.0676	0.0817	0.0682	0.0319
W2/ML	0.0182	0.0171	0.0172	0.0602	0.0843	0.0783	0.0221
W2/MM	0.0181	0.0170	0.0170	0.0508	0.0801	0.0755	0.0198
W3/ML	0.0177	0.0169	0.0158	0.0578	0.0402	0.0296	0.0184
LN2/ML	0.0766	0.0801	0.0784	0.0531	0.0376	0.0410	0.0430
LN2/MM	0.0617	0.0654	0.0644	0.0772	0.0500	0.0482	0.0507
G/ML	0.0428	0.0463	0.0450	0.0502	0.0656	0.0530	0.0194
G/MM	0.0370	0.0398	0.0390	0.0515	0.0717	0.0596	0.0218
GEV/ML	0.0189	0.0195	0.0198	0.0581	0.0768	0.0662	0.0242
GEV/MM	0.0151	0.0162	0.0165	0.0693	0.0842	0.0727	0.0192
LN3/ML	0.0203	0.0206	0.0209	0.0520	0.0711	0.0619	0.0232
LN3/MM	0.0125	0.0132	0.0144	0.0699	0.0858	0.0749	0.0190

GG/ML	0.0160	0.0161	0.0153	0.0446	0.0243	0.0178	0.0141
GG/MM	0.0157	0.0156	0.0157	0.0508	0.0745	0.0649	0.0115
P3/ML	0.0228	0.0232	0.0233	0.0473	0.0250	0.0201	0.0187
P3/MM	0.0123	0.0132	0.0134	0.0641	0.0810	0.0703	0.0146
LP3/GMM	0.0213	0.0217	0.0229	0.0428	0.0685	0.0592	0.0110
KAP/ML	0.0214	0.0220	0.0241	0.0510	0.0245	0.0144	0.0124
KAP/LM	0.0138	0.0141	0.0138	0.0266	0.0119	0.0069	**0.0068**
MWW/LS	**0.0065**	**0.0050**	**0.0073**	**0.0084**	**0.0057**	0.0062	0.0077
MGG/LS	0.0076	0.0126	0.0150	0.0307	0.0122	**0.0045**	**0.0043**
KE	0.0213	0.0211	0.0217	0.0468	0.0318	0.0260	0.0227

x The ln *L* statistic cannot be calculated for this series.
Best statistics are in bold characters.

Table 7. Ranking of D/Ms for different heights for Al Hala based on the goodness-of-fit statistics.

Statistic	Height (m)	Rank of D/Ms 1st	2nd	3rd	4th	5th	6th
ln L							
	40	MWW/LS[2]	W3/ML[1]	GG/ML	GG/MM	MGG/LS	W2/ML
	60	MWW/LS[2]	MGG/LS	W3/ML[1]	GG/ML	GG/MM	W2/ML
	80	MWW/LS[2]	W3/ML[1]	GG/ML	GG/MM	W2/ML	W2/MM
R^2_{PP}							
	40	MGG/LS[2]	MWW/LS	P3/MM[1]	LN3/MM	KAP/LM	W2/ML
	60	MWW/LS[2]	MGG/LS	P3/MM[1]	LN3/MM	KAP/LM	W2/MM
	80	MWW/LS[2]	W2/ML[1]	W2/MM	P3/MM	MGG/LS	KAP/LM
R^2_{QQ}							
	40	MWW/LS[2]	GG/MM[1]	GG/ML	W3/ML	KAP/LM	W2/MM
	60	MWW/LS[2]	GG/MM[1]	GG/ML	W3/ML	W2/ML	W2/MM
	80	MWW/LS[2]	GG/MM[1]	GG/ML	W3/ML	W2/MM	W2/ML
χ^2							
	40	MWW/LS[2]	MGG/LS	GG/ML[1]	GG/MM	W3/ML	W2/MM
	60	MWW/LS[2]	MGG/LS	GG/ML[1]	W3/ML	GG/MM	W2/ML
	80	MWW/LS[2]	W3/ML[1]	GG/ML	GG/MM	MGG/LS	W2/MM
KS							
	40	MWW/LS[2]	MGG/LS	P3/MM[1]	LN3/MM	KAP/LM	GEV/MM
	60	MWW/LS[2]	MGG/LS	LN3/MM[1]	P3/MM	KAP/LM	GG/MM
	80	MWW/LS[2]	P3/MM[1]	KAP/LM	LN3/MM	MGG/LS	GG/ML

[1]best one-component parametric pdf
[2]best mixture parametric pdf

Table 8. Ranking of D/Ms for different heights for Masdar Wind Station based on the goodness-of-fit statistics.

Statistic	Height (m)	Rank of D/Ms 1st	2nd	3rd	4th	5th	6th
ln L							
	10	MWW/LS[b]	MGG/LS	KAP/ML[a]	P3/ML	GG/ML	LP3/GMM
	30	MWW/LS[b]	MGG/LS	KAP/ML[a]	GG/ML	P3/ML	LP3/GMM
	40	MGG/LS[b]	MWW/LS	KAP/ML[a]	GG/ML	P3/ML	LP3/GMM
	50	MGG/LS[b]	LP3/GMM[a]	KAP/ML	GG/ML	GG/MM	P3/ML
R^2_{PP}							
	10	MWW/LS[b]	KAP/LM[a]	MGG/LS	KE	LP3/GMM	LNb/ML
	30	MWW/LS[b]	MGG/LS	KAP/LM[a]	KE	KAP/ML	P3/ML
	40	MGG/LS[b]	MWW/LS	KAP/LM[a]	KAP/ML	GG/ML	P3/ML
	50	MGG/LS[b]	MWW/LS	KAP/LM[a]	LP3/GMM	KAP/ML	GG/MM
R^2_{QQ}							
	10	MWW/LS[b]	MGG/LS	KAP/LM[a]	LP3/GMM	KE	GG/MM
	30	MGG/LS[b]	MWW/LS	KAP/LM[a]	KAP/ML	KE	W3/ML
	40	MWW/LS[b]	KAP/ML[a]	MGG/LS	KAP/LM	GG/ML	W3/ML
	50	MGG/LS[b]	GG/MM[a]	GG/ML	LP3/GMM	KAP/ML	P3/MM
χ^2							
	10	MWW/LS[b]	KAP/LM[a]	MGG/LS	KE	KAP/ML	LP3/GMM
	30	MWW/LS[b]	MGG/LS	KAP/LM[a]	KAP/ML	P3/ML	GG/ML
	40	MGG/LS[b]	KAP/LM[a]	KAP/ML	MWW/LS	GG/ML	P3/ML
	50	MGG/LS[b]	LP3/GMM[a]	KAP/ML	GG/ML	GG/MM	KAP/LM
KS							
	10	MWW/LS[b]	KAP/LM[a]	MGG/LS	LP3/GMM	GG/ML	KE
	30	MWW/LS[b]	KAP/LM[a]	MGG/LS	GG/ML	KAP/ML	P3/ML
	40	MGG/LS[b]	MWW/LS	KAP/LM[a]	KAP/ML	GG/ML	P3/ML
	50	MGG/LS[b]	KAP/LM[a]	MWW/LS	LP3/GMM	GG/MM	KAP/ML

[a]best one-component parametric pdf
[b]best mixture parametric pdf

Figure captions

Figure 1. Geographical location of the meteorological stations.

Figure 2. Example of a) P-P plot and b) Q-Q plot for the case for KAP/LM at the station of East Jebel Haffet.

Figure 3. Median wind speed of stations at 10 m height.

Figure 4. Altitude of stations at 10 m height.

Figure 5. Box plots of statistics for stations at 10 m height: a) R_{PP}^2, b) R_{QQ}^2, c) χ^2 and d) KS.

Figure 6. Frequency histograms and normal probability plots of wind speed for the stations at 10 m height. The fitted pdfs of the W2/MM, KAP/LM, MWW/LS and KE are superimposed.

Figure 7. Box plots of statistics for Al Hala: a) R_{PP}^2, b) R_{QQ}^2, c) χ^2 and d) KS.

Figure 8. Box plots of statistics for Masdar Wind Station: a) R_{PP}^2, b) R_{QQ}^2, c) χ^2 and d) KS.

Figure 9. Frequency histograms and normal probability plots of wind speed for Al Hala at 40 m, 60 m and 80 m heights. The fitted pdfs of the W2/MM, KAP/LM, MWW/LS and KE are superimposed.

Figure 10. Frequency histograms and normal probability plots of wind speed for Masdar Wind Station at 10 m, 30 m, 40 m and 50 m heights. The fitted pdfs of the W2/MM, KAP/LM, MWW/LS and KE are superimposed.

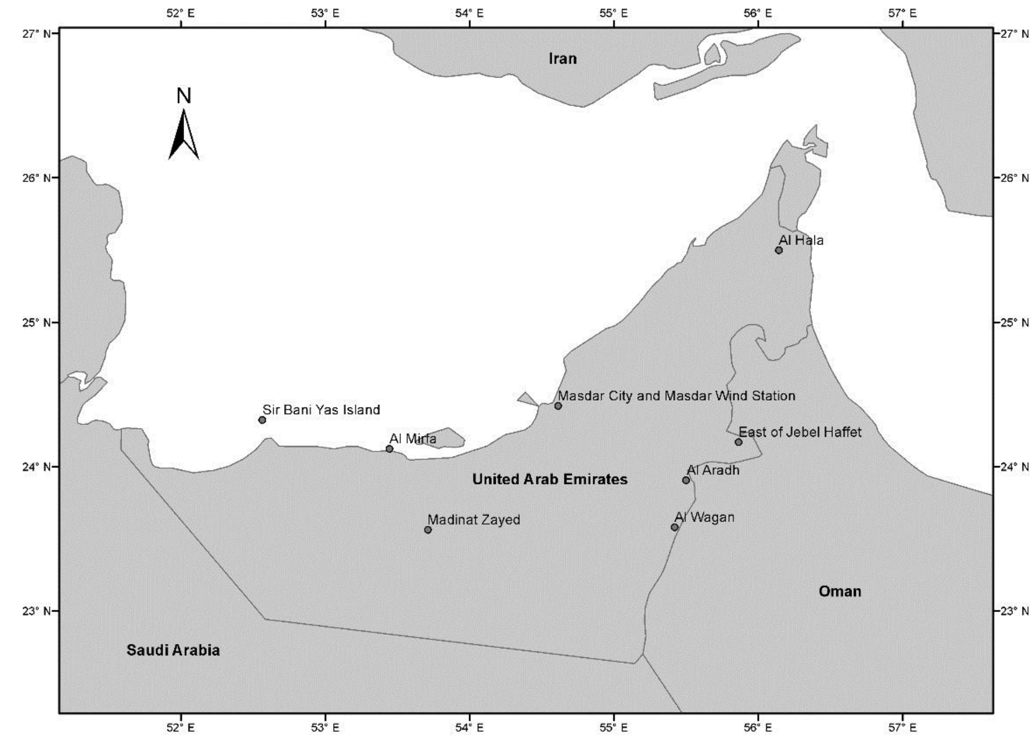

Figure 1. Geographical location of the meteorological stations.

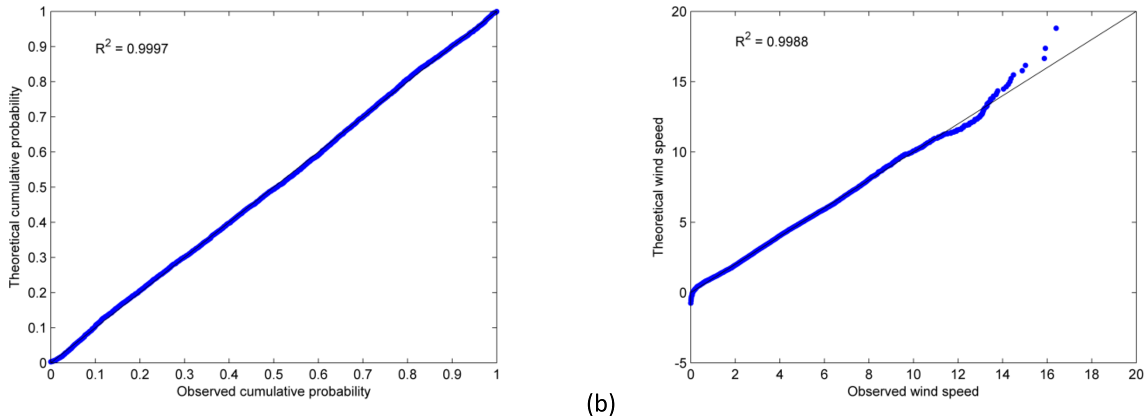

Figure 2. Example of a) P-P plot and b) Q-Q plot for the case for KAP/LM at the station of East Jebel Haffet.

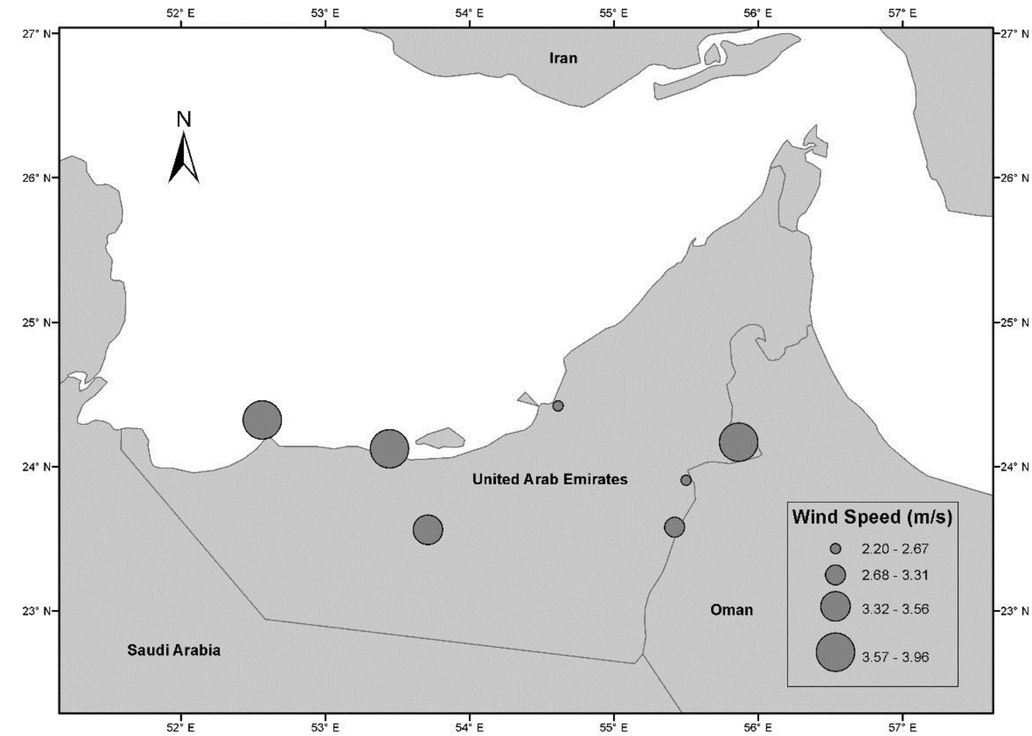

707

708 Figure 3. Median wind speed of stations at 10 m height.

709

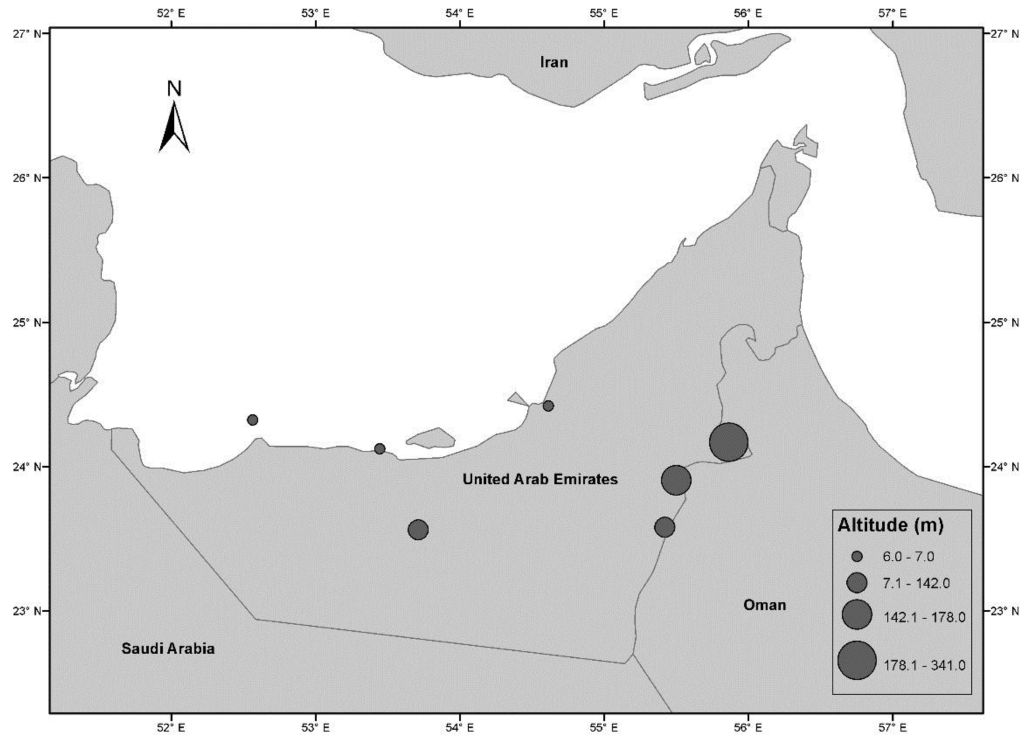

Figure 4. Altitude of stations at 10 m height.

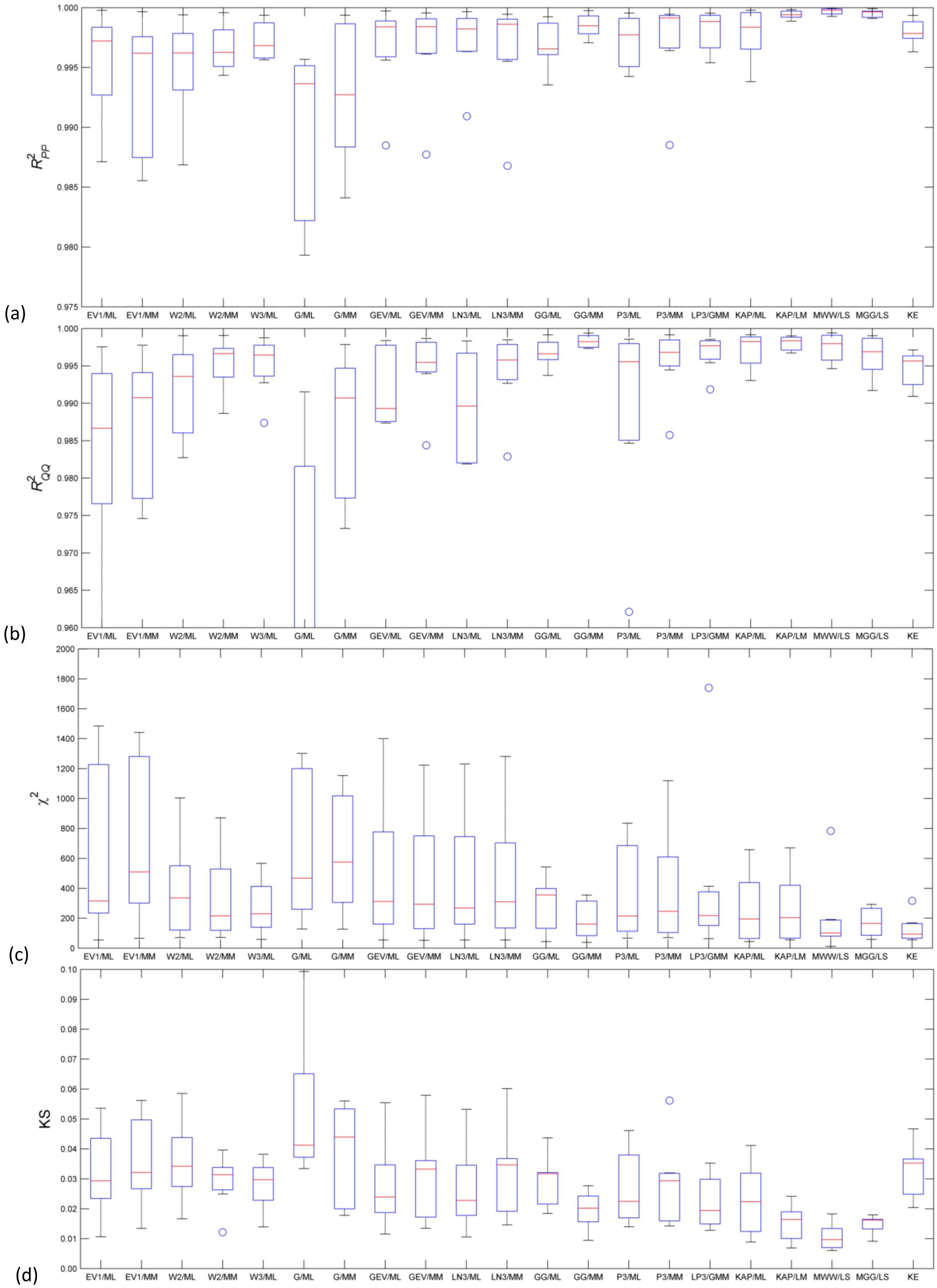

Figure 5. Box plots of statistics for stations at 10 m height: a) R_{PP}^{2} , b) R_{QQ}^{2} , c) χ^{2} and d) KS.

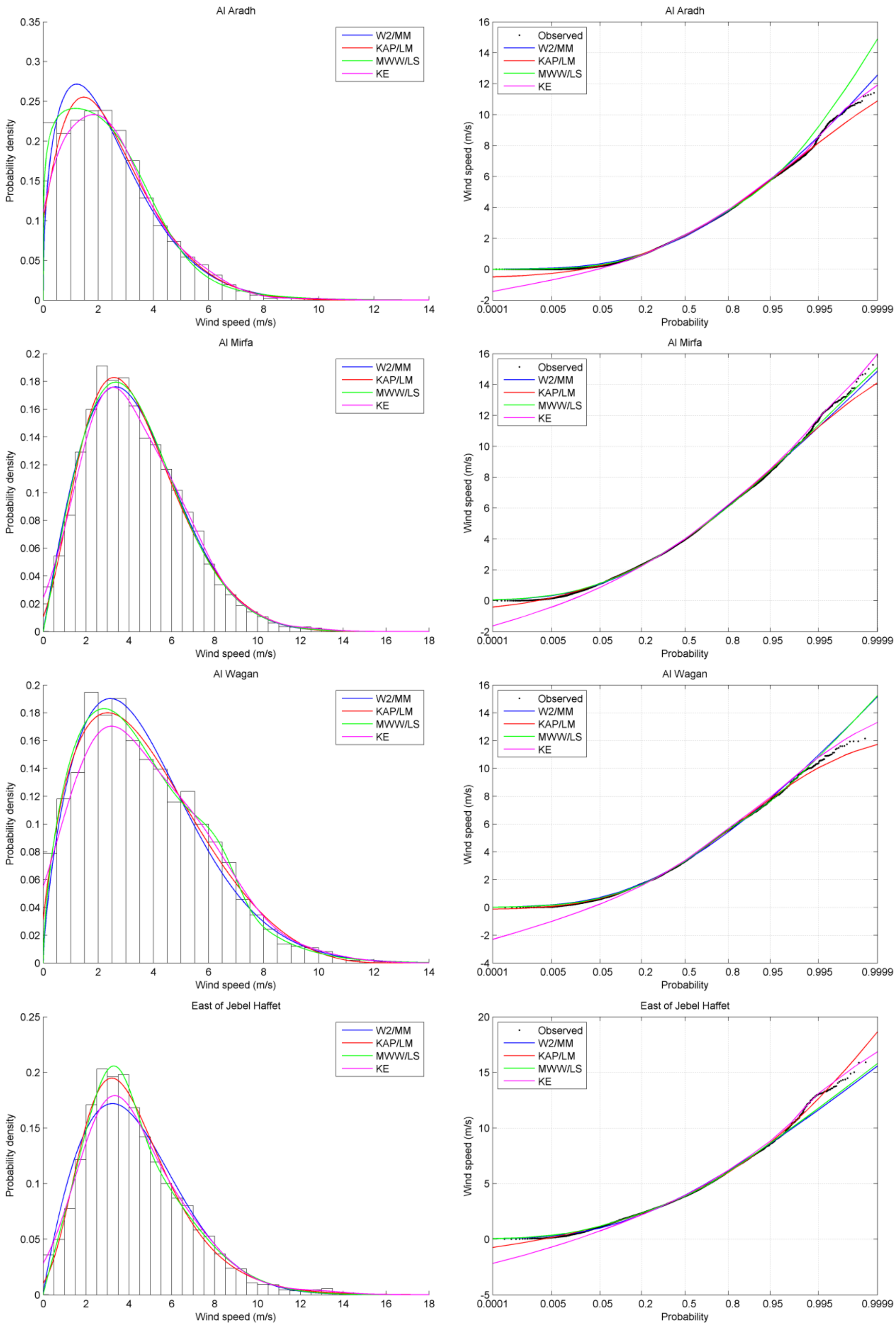

Figure 6. Frequency histograms and normal probability plots of wind speed for the stations at 10 m height. The fitted pdfs of the W2/MM, KAP/LM, MWW/LS and KE are superimposed.

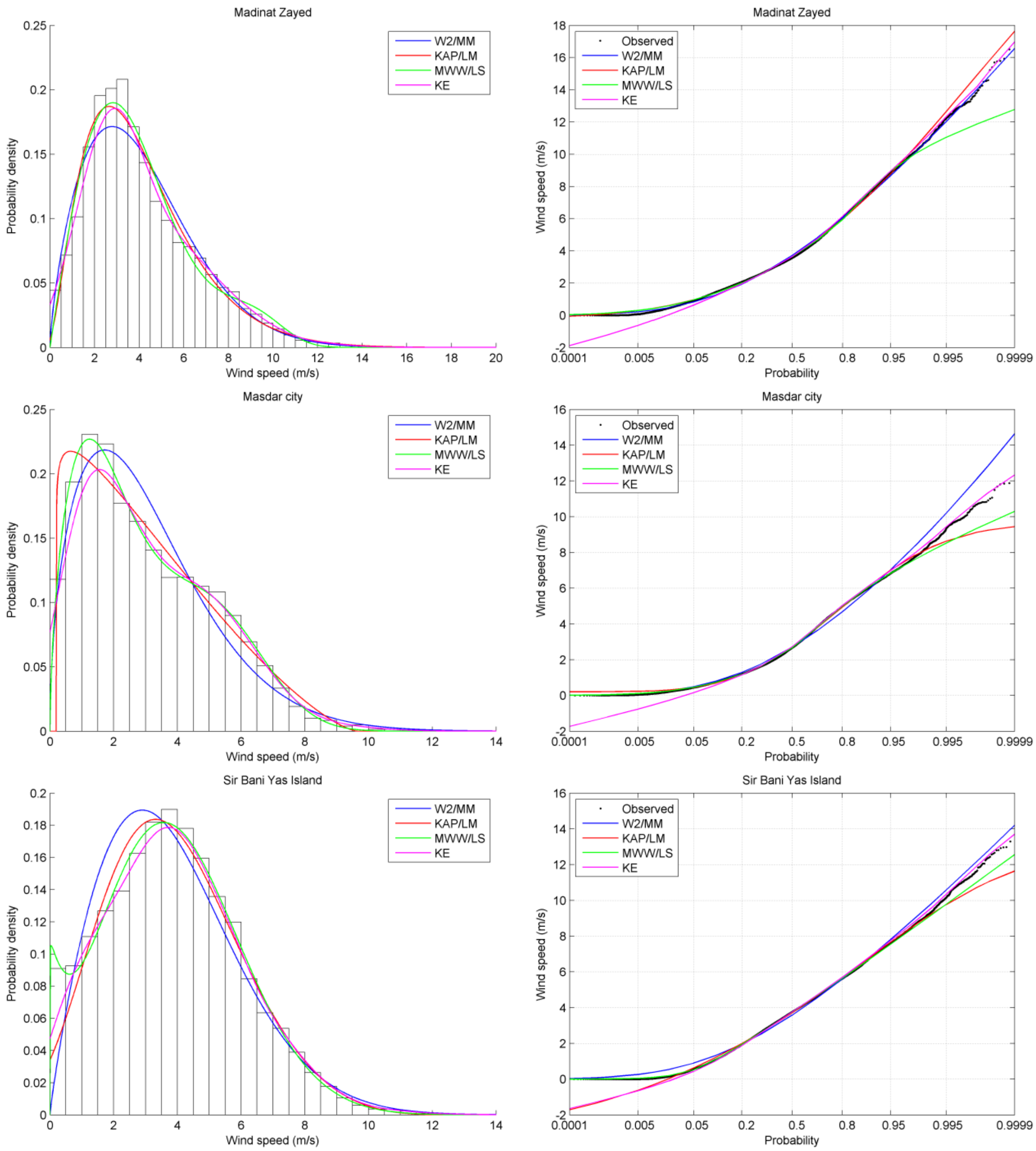

Figure 6. Frequency histograms and normal probability plots of wind speed for the stations at 10 m height. The fitted pdfs of the W2/MM, KAP/LM, MWW/LS and KE are superimposed. (continued)

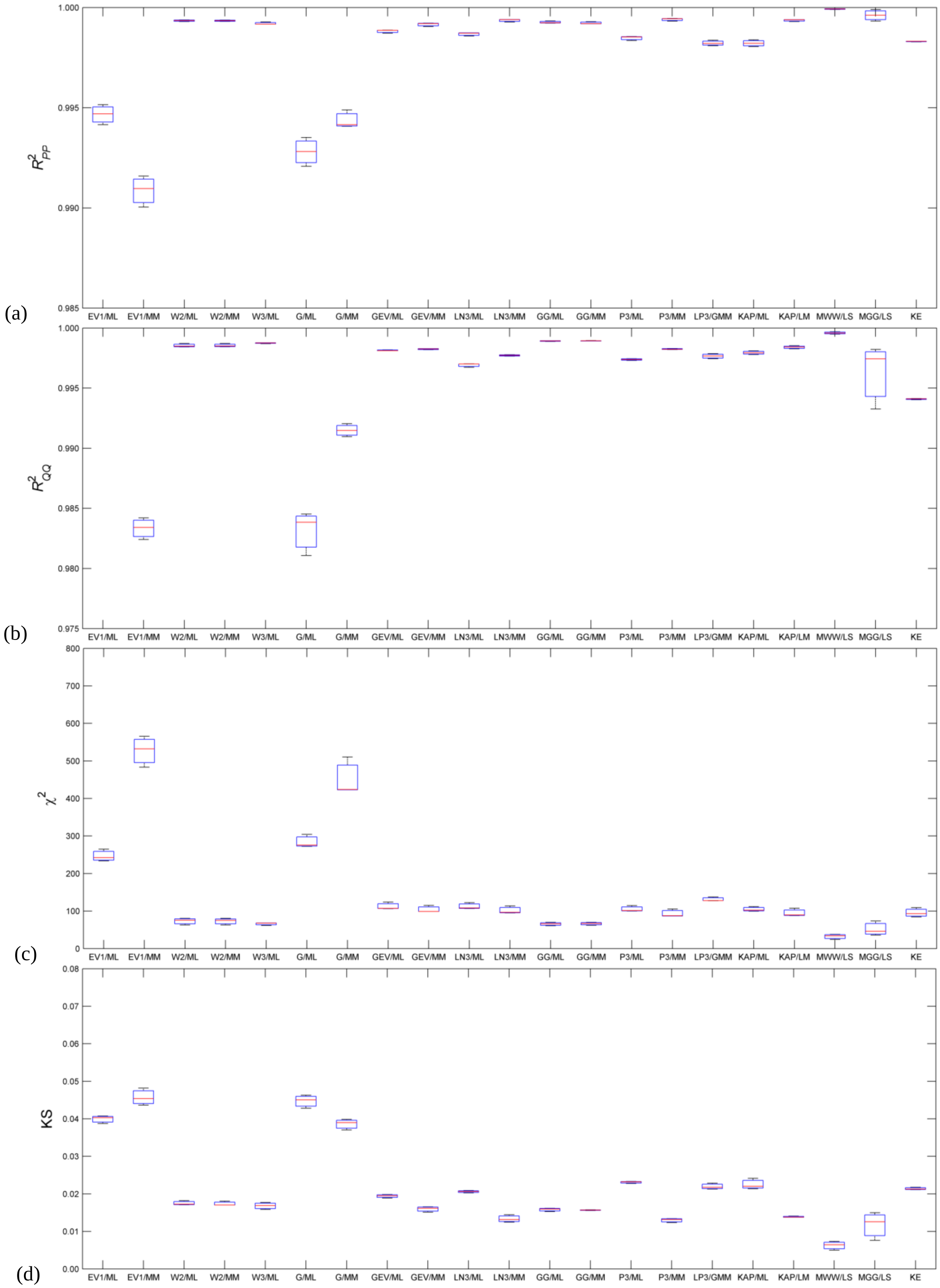

Figure 7. Box plots of statistics for Al Hala: a) R^2_{PP}, b) R^2_{QQ}, c) χ^2 and d) KS.

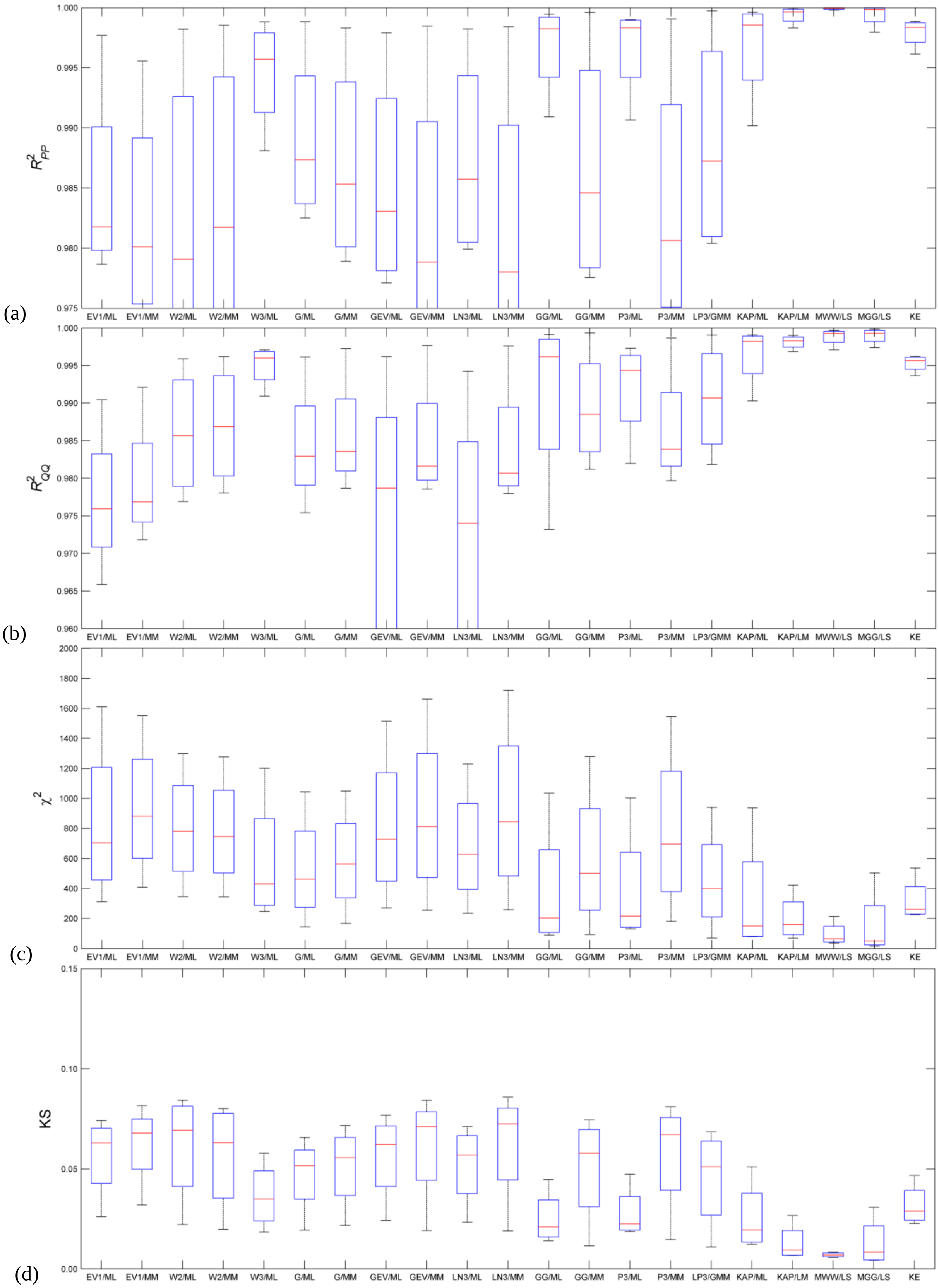

Figure 8. Box plots of statistics for Masdar Wind Station: a) R_{PP}^2, b) R_{QQ}^2, c) χ^2 and d) KS.

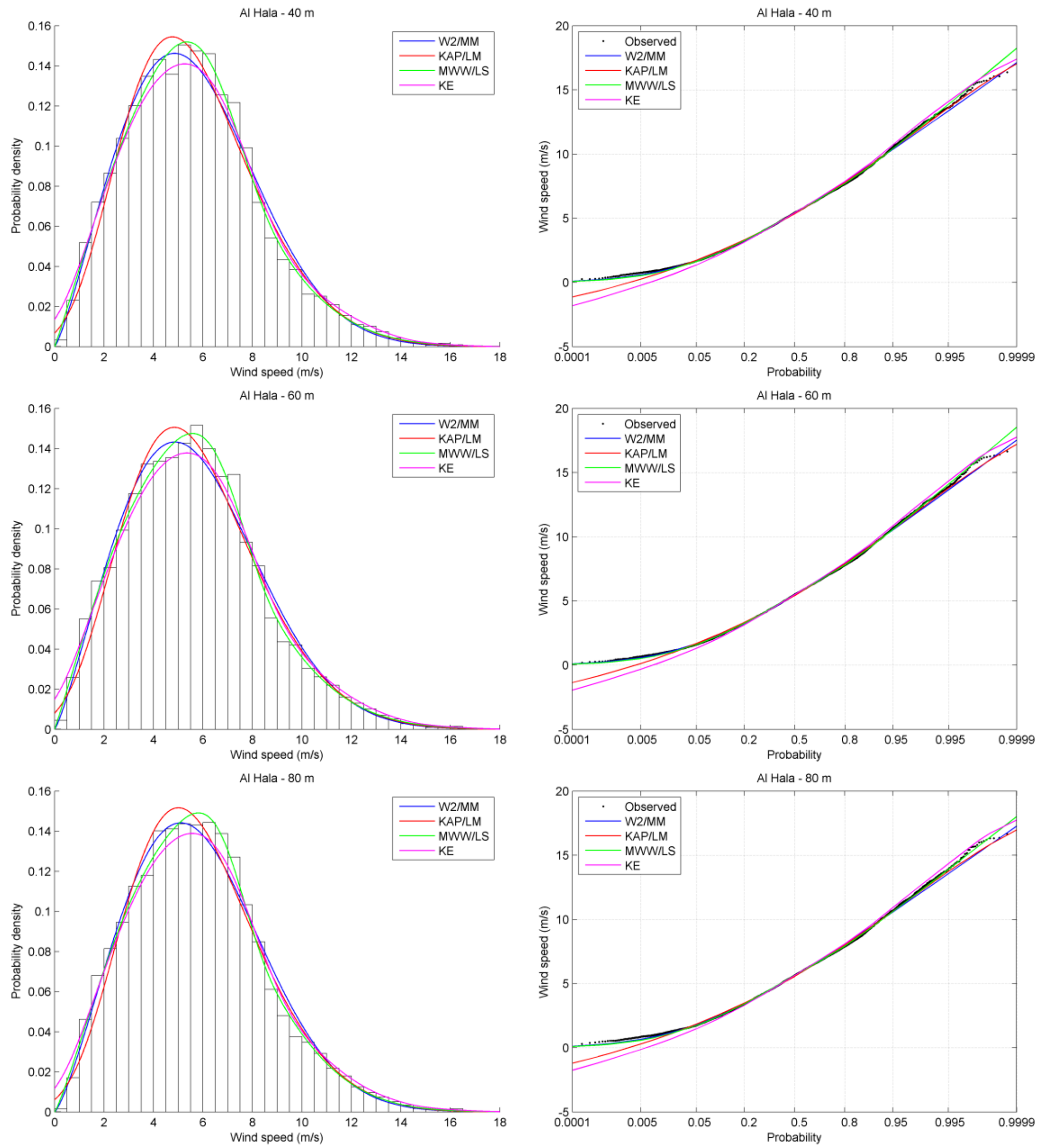

Figure 9. Frequency histograms and normal probability plots of wind speed for Al Hala at 40 m, 60 m and 80 m heights. The fitted pdfs of the W2/MM, KAP/LM, MWW/LS and KE are superimposed.

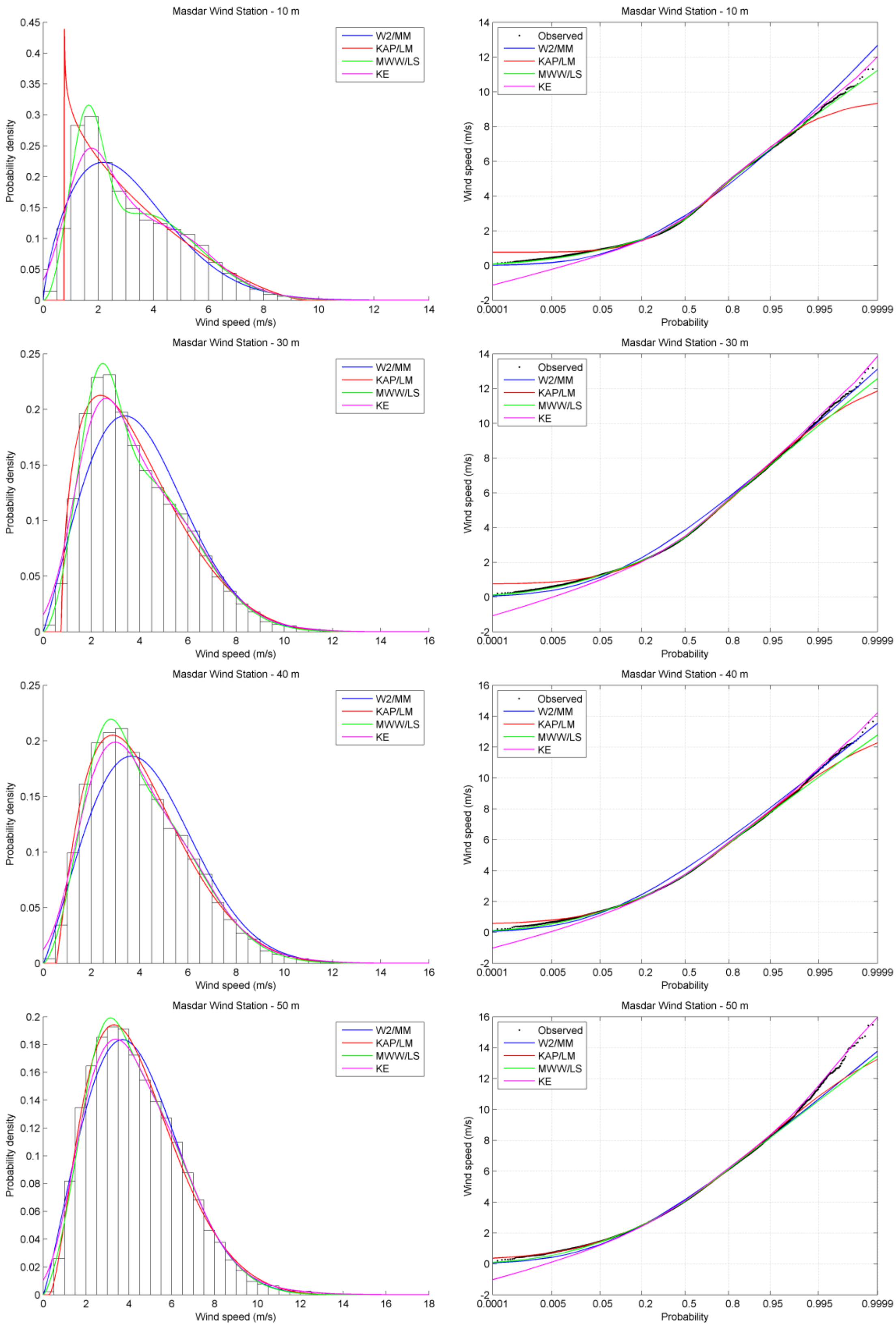

Figure 10. Frequency histograms and normal probability plots of wind speed for Masdar Wind Station at 10 m, 30 m, 40 m and 50 m heights. The fitted pdfs of the W2/MM, KAP/LM, MWW/LS and KE are superimposed.